CRC Project No. CM-138-15-1

Development of a Thermodynamics-Based Fundamental Model for Prediction of Gasoline/Ethanol Blend Properties and Vehicle Driveability

May 2016

COORDINATING RESEARCH COUNCIL, INC.
5755 NORTH POINT PARKWAY·SUITE 265·ALPHARETTA, GA 30022

The Coordinating Research Council, Inc. (CRC) is a non-profit corporation supported by the petroleum and automotive equipment industries. CRC operates through the committees made up of technical experts from industry and government who voluntarily participate. The four main areas of research within CRC are: air pollution (atmospheric and engineering studies); aviation fuels, lubricants, and equipment performance, heavy-duty vehicle fuels, lubricants, and equipment performance (e.g., diesel trucks); and light-duty vehicle fuels, lubricants, and equipment performance (e.g., passenger cars). CRC's function is to provide the mechanism for joint research conducted by the two industries that will help in determining the optimum combination of petroleum products and automotive equipment. CRC's work is limited to research that is mutually beneficial to the two industries involved. The final results of the research conducted by, or under the auspices of, CRC is available to the public.

CRC makes no warranty expressed or implied on the application of information contained in this report. In formulating and approving reports, the appropriate committee of the Coordinating Research Council, Inc. has not investigated or considered patents, which may apply to the subject matter. Prospective users of the report are responsible for protecting themselves against liability for infringement of patents.

CRC Project No. No. CM-138-15-1

Development of a Thermodynamics-Based Fundamental Model for Prediction of Gasoline/Ethanol Blend Properties and Vehicle Driveability

Submitted by

Sam Reddy
Evap Consulting, Inc.
Sam.r.reddy@ReddyEvap.com
May 16, 2016

Development of a Thermodynamics-Based Fundamental Model for Prediction of Gasoline/Ethanol Blend Properties and Vehicle Driveability

Abstract

Cold-start and warm-up driveability performance of gasoline-fueled vehicles correlates with fuel driveability index (DI) which is estimated from ASTM distillation temperatures (DI = 1.5*T10+3*T50+T90). Vehicle driveability performance is inversely proportional to DI. Ethanol in gasoline decreases DI by depressing T50, but vehicle driveability performance is not improved. In previous CRC studies, empirical ethanol correction factors were added to the DI equation without understanding the full effect of ethanol on driveability. The purpose of this study was to develop a fundamental thermodynamic model for understanding the ethanol effect on cold-start and warm-up driveability to develop a better equation for driveability index that would model a wider range of ethanol concentrations in gasoline. A thermodynamic model was developed for predicting fuel vaporization in cold engine combustion systems as a function of ethanol concentration in the fuel. The model showed that the T50 depression (ΔT50) by ethanol is a misleading indicator of driveability improvement; therefore, a modified driveability index $DI_{\Delta T50}$ is proposed ($DI_{\Delta T50}$=1.5*T10+3*T50+T90+ 3*ΔT50), which correlates well with the CRC-666 study published driveability data. The second goal of the study was to develop equations for estimating T50 depression (ΔT50) of any given ethanol blend from its commonly measured fuel properties. A simple equation for estimating average ΔT50 as a function of ethanol concentration and more complex equations for estimating ΔT50 as a function ethanol concentration and the blend T50 were developed.

Introduction

Vehicle cold-start and warm-up driveability (hereinafter called driveability) problems arise due to insufficient fuel vaporization in cold engine combustion systems. These driveability problems continue until the fuel-facing surfaces of the combustion system have warmed and more fuel vaporizes. Several studies were previously conducted to determine the relationship between gasoline ASTM D86 distillation temperatures and the resultant driveability [1-8]. It was determined that the mid-range boiling point T50 (50% distilled point) was the most important of three distillation points (T10, T50 and T90) and an equation to predict driveability Index (DI) was developed and successfully implemented for hydrocarbon fuels [1].

$$DI \text{ (hydrocarbon fuels only)} = 1.5*T10 + 3.0*T50 + T90 \quad (1)$$

High DI (e.g., DI >1250°F) of a fuel is an indication of poor driveability. It was found that adding ethanol (up to 20%) to gasoline decreases DI by depressing T50, which implies better driveability with gasoline-ethanol blends than with gasoline alone; however, the test data showed little or no driveability improvement. Therefore, CRC subsequently conducted two test programs to determine a correction to the DI equation for ethanol blends [2, 3]:

$$DI \text{ (E0 - E10)} = 1.5*T10 + 3.0*T50 + T90 + 2.4*EtOH \quad (2)$$

$$DI \text{ (E15 - E20)} = 1.5*T10 + 3.0*T50 + T90 + 9.49*EtOH \quad (3)$$

where E0, E10, E15, and E20 are gasoline-ethanol blends containing 0, 10, 15, and 20 vol % ethanol, respectively; EtOH is the volume percent ethanol in a gasoline-ethanol blend. In further discussion, the uncorrected DI estimated by using Equation (1) will be denoted as DI or DI_{E0} and the corrected DIs estimated by using Equations (2) and (3) will be denoted as DI_{E10} and DI_{E20}, respectively. Also, in further discussion, a fuel blend always refers to a gasoline-ethanol blend or an ethanol-containing gasoline.

As ethanol concentration in gasoline increases above 10 vol % there are concerns that potential errors in the ethanol correction to the DI equation are increasing and that the brute-force regression approach is not a very desirable method of understanding ethanol effects and predicting driveability. Therefore, CRC initiated the current project

to conduct a more fundamental evaluation of the ethanol effect on driveability that would yield better results.

The objectives of the project were:

1. To develop a thermodynamic model to predict fuel vaporization during cold-start and warm-up under cool ambient conditions to understand the effects of ethanol.
2. To review past CRC and any other studies on the driveability performance of vehicles with gasoline and gasoline-ethanol blends and, thereby, develop a better model for predicting driveability index of gasoline-ethanol blends.

As indicated earlier, cold-start and warm-up driveability problems are due to insufficient fuel vaporization in cold engine combustion systems. Therefore, the purpose of an intended thermodynamic model for this study was to predict fuel vaporization in a cold engine combustion system as a function of ethanol concentration in the fuel. Such a model can help us understand why the DIs of ethanol blends do not correlate well with vehicle driveability performance. Once the theory and mechanism of ethanol effects on cold-start and warm-up is understood, a better model can be developed for predicting driveability index of ethanol blends.

Low concentrations of ethanol (up to 20%) in gasoline affect blended fuel properties which relate to fuel vaporization and driveability as follows:

1. Increased fuel vapor pressure occurs because ethanol forms a non-ideal solution with gasolines [9, 10], which can positively affect blended fuel vaporization during cold-start and warm-up. Note that pure ethanol vapor pressure DVPE (Dry Vapor Pressure Equivalent) is low (2.4 psi) compared to gasoline vapor pressures (7-15 psi); therefore, it should decrease blended fuel DVPE if it formed an ideal solution.
2. Increased heat of vaporization (HOV) and subsequent charge cooling (i.e., a decrease in fuel/air mixture temperature) [11] results because of the higher HOV of ethanol (840 KJ/kg) compared to the HOV of gasoline (approximately 305 KJ/kg), which can negatively affect blended fuel vaporization during cold-start and warm-up.

3. Increased lower flammability limit (LFL) of vapors [12] because of the higher LFL of ethanol (3.3 vol % in air) compared to the LFL of gasoline (1.4 vol % in air), which can negatively affect cold-start and warm-up with ethanol blends.

The intended thermodynamic model for fuel vaporization should take into account all these effects of ethanol to predict the performance of ethanol blends during vehicle cold-start and warm-up. Note that modern vehicle engine combustion systems can be PFI (Port Fuel Injection) or DI (Direct Injection); however, the combustion system in this study refers to a generic combustion system as illustrated in the next section. It was beyond the scope of this project to study the differences in fuel vaporization between PFI and DI systems.

Thermodynamic Model for Predicting Fuel Vaporization in Cold Engine Combustion Systems

Figure 1 shows the schematic of the fuel vaporization process in a generic cold engine combustion system. A small amount of fuel (about 0.1 to 0.2 cc of fuel per liter of air) is injected into the cold engine combustion system. Under cold-start and warm-up conditions, only a portion of the fuel vaporizes depending on the temperature and fuel composition. If a sufficient quantity of fuel vaporizes, the engine will not experience any driveability problems.

Figure 1. Schematic of fuel vaporization in a combustion system

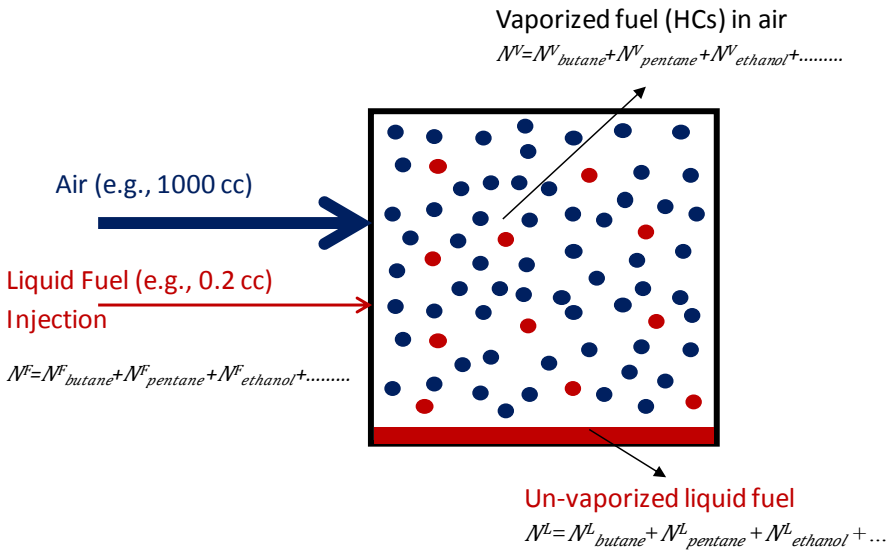

Fuel is a mixture of hundreds of different hydrocarbons and ethanol. Fuel vaporization in a cold engine combustion system can be estimated by using the modified Raoult's Law [13] for vapor-liquid equilibrium of each fuel component i:

$$\Phi_i \, p_i = \gamma_i \; x_i \; P_i \quad (i=\text{butane, pentane, ethanol, ...}) \tag{1}$$

where Φ_i is the fugacity coefficient, p_i is the partial pressure of component i in the gas mixture, γ_i is the activity coefficient, x_i is the mole fraction of component i in the un-vaporized liquid, and P_i is pure component vapor pressure.

The partial pressure of component i, p_i is proportional to the gram moles of component i in the vapor phase (N^V_i). From the ideal gas law:

$$p_i \, V = N^V_i \, RT \tag{2}$$

where V is gas space volume, R is the ideal gas law constant, and T is temperature.

The mole fraction of component i, x_i in un-vaporized liquid fuel is given by:

$$x_i = N^L_i \,/\, (N^L_{butane} + N^L_{pentane} + N^L_{ethanol} + ...) \tag{3}$$

where N^L_i is gram moles of component i in un-vaporized liquid fuel. Similarly, all other terms in Equation (3) correspond to the other fuel components as shown in Figure 1.

From Equations (1) and (2):

$$N^V_i = (V/RT) \, \gamma_i \; x_i \; P_i \,/ \Phi_i \tag{4}$$

The pure component vapor pressure P_i is computed using the Antoine vapor pressure equation (14):

$$\log_{10} P_i = A - B/(T-C) \tag{5}$$

where T is temperature in K; and A, B, and C are characteristic constants of each component (e.g., for ethanol $A= 8.1122$, $B= 1592.86$, and $C= 46.97$) [14].

The activity coefficient γ_i is a factor used in thermodynamics to account for liquid phase deviations from ideal behavior in a mixture of chemical substances. Ethanol and

gasoline form non-ideal mixtures; therefore, the estimation of the ethanol activity coefficient is extremely important. In this study, UNIFAC (Universal Quasi-Chemical Functional Group Activity Coefficients) theory [9,15] was used for estimating the activity coefficients of fuel components. The basic idea of this approach is that a physical property of an organic molecule is the sum of the contributions made by each of the molecule's functional groups. The functional groups are structural units, which combine to form the parent molecule. For example, n-butane is made of two CH_3 and two CH_2 groups. The usefulness of this approach lies in the fact that the number of functional groups that constitute various fuel compounds is a small number compared to the number of compounds, which are made up of these groups. Therefore, by using the properties or parameters of only a small number of functional groups, it is possible to estimate the thermodynamic properties of multicomponent mixtures including gasoline-ethanol blends. The model [9] has proven capable of predicting the vapor pressures and vapor compositions of any oxygenated fuel.

The fugacity coefficient of component i, Φ_i is a factor used in thermodynamics to account for gas phase deviations from ideal gas behavior and it is estimated by using the Redlich-Kwong equation of state [13]. Unlike activity coefficients, fugacity coefficients are not very important for this study because gas phase deviation from ideal gas law is negligible.

As fuel vaporizes, its latent heat of vaporization (*HOV*) causes charge cooling (i.e., a decrease in fuel/air mixture temperature), which reduces the amount of fuel vaporizing in the combustion system. Therefore, as the injected fuel starts to vaporize in the combustion chamber, its composition is changing as lighter hydrocarbons are vaporizing preferentially because of their higher vapor pressure, and its temperature is decreasing because of the latent heat of vaporization. These processes will continue until both thermodynamic vapor-liquid equilibrium and adiabatic thermal equilibrium are achieved. From an energy balance:

$$\sum HOV_i N^V_i = (m_{fuel}C_{pfuel}+m_{air}C_{pair})\Delta T \qquad (6)$$

where $\sum HOV_i N^V_i = HOV_{butane} N^V_{butane} + HOV_{pentane} N^V_{pentane} + HOV_{ethanol} N^V_{ethanol} + \ldots\ldots\ldots$ where HOV_i is the heat of vaporization of component i; m_{fuel} and m_{air} are the mass of fuel and air respectively; C_{pfuel} and C_{pair} are the heat capacities of fuel and air respectively; and ΔT is the adiabatic cooling of fuel and air.

The Heats of vaporization of the fuel components were calculated using the following equation [11]:

$$HOV = RT_c[7.08(1-T_r)^{0.354} + 10.95\omega(1-T_r)^{0.456}] \quad (7)$$

where R = 0.008314 kJ/mole K ideal gas law constant; $T_r = T / T_c$ where T_c is critical temperature; and ω is the acentric factor of fuel component.

There are three unknowns and three equations with which to solve for those unknowns as summarized below.

Three unknowns:

1. Vapor composition: $N^V = N^V_{butane} + N^V_{pentane} + N^V_{ethanol} + \ldots\ldots\ldots$
2. Un-vaporized liquid fuel composition: $N^L = N^L_{butane} + N^L_{pentane} + N^L_{ethanol} + \ldots\ldots\ldots$
3. Adiabatic charge cooling: ΔT

Three equations:

1. Modified Raoult's Law equation: $N^V_i = (V/RT)\,\gamma_i\, x_i\, P_i / \Phi_i$
2. Mass balance of each component: $N^F_i = N^V_i + N^L_i$
3. Energy balance: $\sum HOV_i N^V_i = (m_{fuel}C_{pfuel} + m_{air}C_{pair})\Delta T$

An iterative numerical method was developed to determine equilibrium vapor composition and fuel vaporization as illustrated in the following schematic diagram (Figure 2) and flow chart (Figure 3). The incremental fuel vaporization illustrated in the first part of Figure 2 is mainly for computing fuel vaporization and vapor-liquid equilibrium. As illustrated in the second part of Figure 2, fuel/air mixture concentration is assumed to be uniform in the combustion chamber. The model is applicable to any

Figure 2. Schematic of iterative method for predicting fuel vaporization in a combustion system

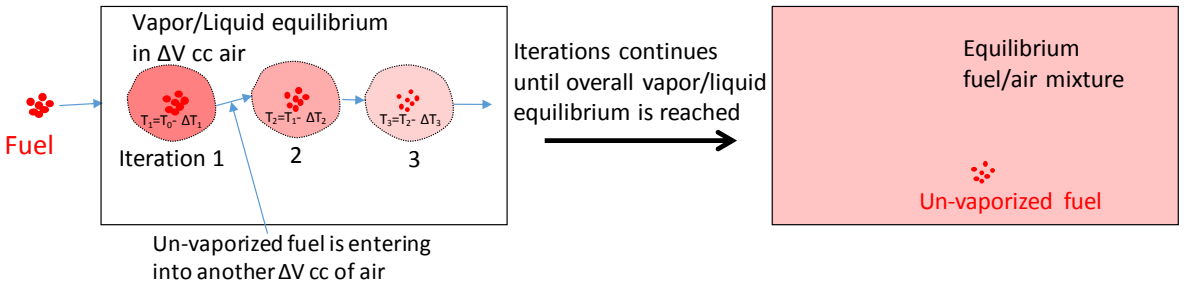

Figure 3. Flow chart of iterative numerical method for predicting fuel vaporization in a combustion system

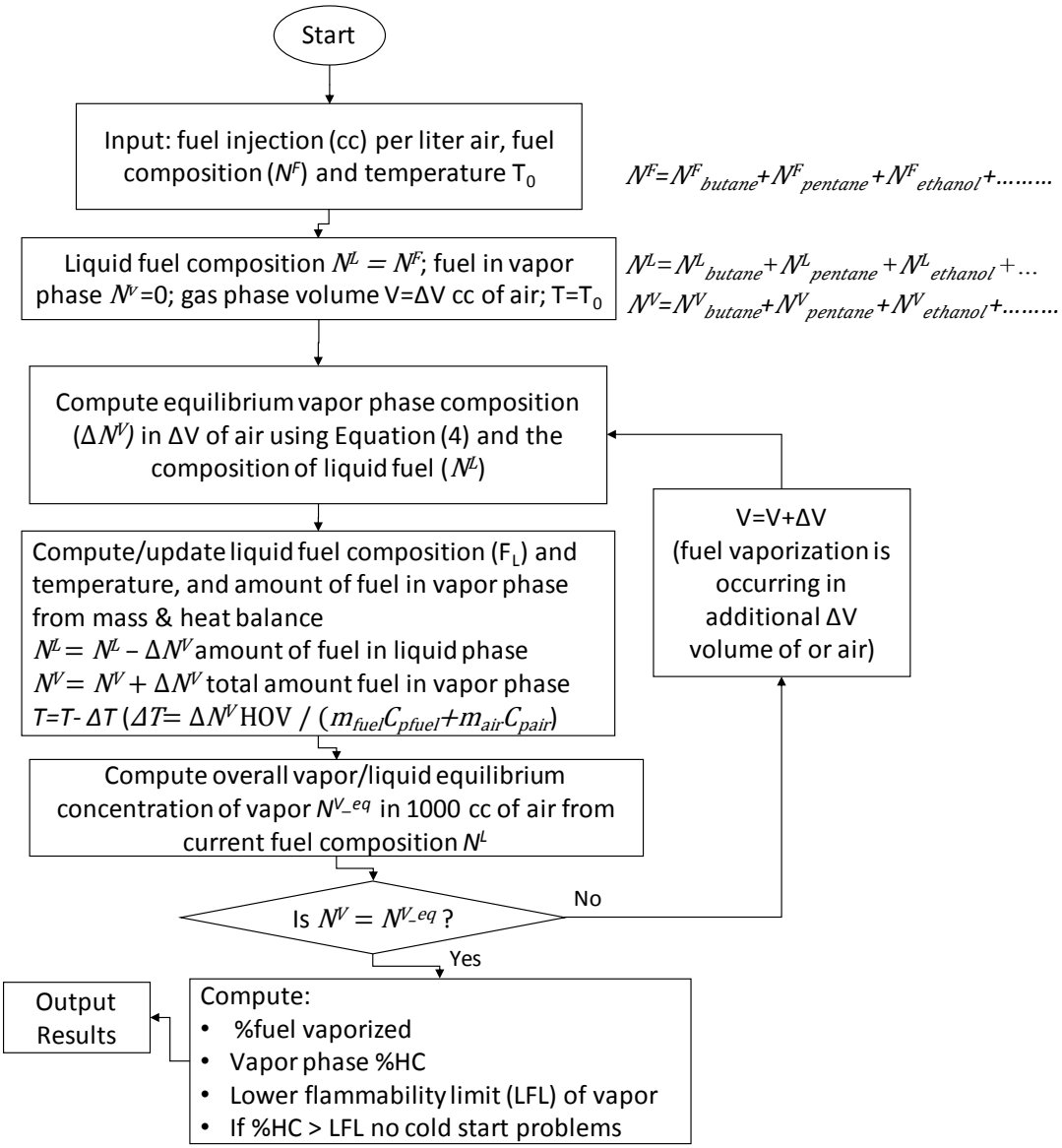

size combustion chamber; however, for convenience all calculations were done by using a combustion chamber volume V=1000 cc and incremental step volume ΔV=1 cc.

After estimating the equilibrium vapor composition, the lower flammability limit (LFL) of the vapor was estimated by using Le Chatelier's mixing rule [12]. The lower flammability limit is the lowest concentration (vol %) of gaseous fuel in air which is capable of producing a propagating flame by an ignition source. At concentrations below the LFL limit, there is not enough hydrocarbon in the fuel-air mixture to start a propagating flame.

A computer program called CRCdriveability was written in C-language using Microsoft Visual C++ 6.0 for executing the calculation steps shown in the algorithm flow chart (Figure 3). As indicated earlier, the main purpose of the thermodynamic model (CRCdriveability program) was to predict fuel vaporization in a cold engine combustion system as a function ethanol concentration in the fuel. The model-predicted fuel vaporization trends were compared with ASTM distillation temperatures and driveability performance data to understand the mechanism of the ethanol effects and develop a better model for estimating driveability index. This objective was achieved by using the thermodynamic model to analyze the fuels used in the 2003 and the 2013 CRC cold-start and warm-up driveability test programs (CRC Reports 638 and 666 or CRC-638 and CRC-666) [2,3]. Chevron provided detailed hydrocarbon analyses of CRC-638 and CRC-666 fuels and fuel composition data files suitable for the program were prepared as described in Appendix A.

Step by step instructions and illustrations, and screen shots of the computer program are shown in Appendix B. For a given fuel, fuel injection amount (cc per liter air), and temperature, the program predicts percent fuel vaporization using the thermodynamic vapor/liquid equilibrium model. After the percent fuel vaporization is computed iteratively, the program computes mass air/fuel ratio of the vapor, and flammability of the vapor. As seen in the later sections of the report, the most useful output from the program for this project was the percent fuel vaporization. Other predicted quantities (flammability, air/fuel ratio, etc.) were not needed in the analysis; however, they are useful to understand the effects of ethanol on cold-start and warm-up driveability.

Thermodynamic Model Verification

The pure component fuel hexane was used to verify the accuracy of the thermodynamic model. For a given temperature (for example 0°F), the model will go through the iterative method and estimate how much hexane will vaporize in the cold engine combustion system. For example, the model predicted fuel vaporization of hexane at 0°F (isothermal) and injection of 0.3 cc fuel/liter air was 46.2%. Using the pure component vapor pressure of hexane which is 0.336 psi at 0°F, the amount of hexane present in 1 liter of hexane saturated air can be estimated by using the ideal gas law equation n/V = P/RT, which is 0.00109078 gmole/liter or 0.094 g/liter. The amount of injected hexane is 0.204 g (0.3 cc*density 0.68 g/cc) per liter of air; therefore, the percent hexane vaporized is 46.1% (100*0.094/0.204) based on pure component vapor pressure. These calculations were repeated at several temperatures and the results are compared in Figure 4. Excellent agreement between both the methods indicates that the thermodynamic model is computing the fuel vaporization correctly. Note that it was possible to verify the model only for isothermal fuel vaporization (without any charge cooling due to heat of vaporization). The next step is to verify the model estimation of heat of vaporization and charge cooling.

The National Renewable Energy Laboratory (NREL) [11] studied the HOV of ethanol blended fuels and their charge cooling. Therefore, the accuracy of model estimated HOV and charge cooling were verified by comparing the predicted results with NREL data and calculations. Table 1 compares HOV and charge cooling estimated by the model with NREL data and calculations for E0, E10, and E20 ethanol blends. The results in Table 1 show an excellent agreement indicating that the model calculations are accurate. Note that the base fuel used in the model calculations was CRC-666 fuel B0 and it was different from the base fuel used in the NREL calculations; however, the NREL study [11] found that HOV is nearly the same to all base fuels.

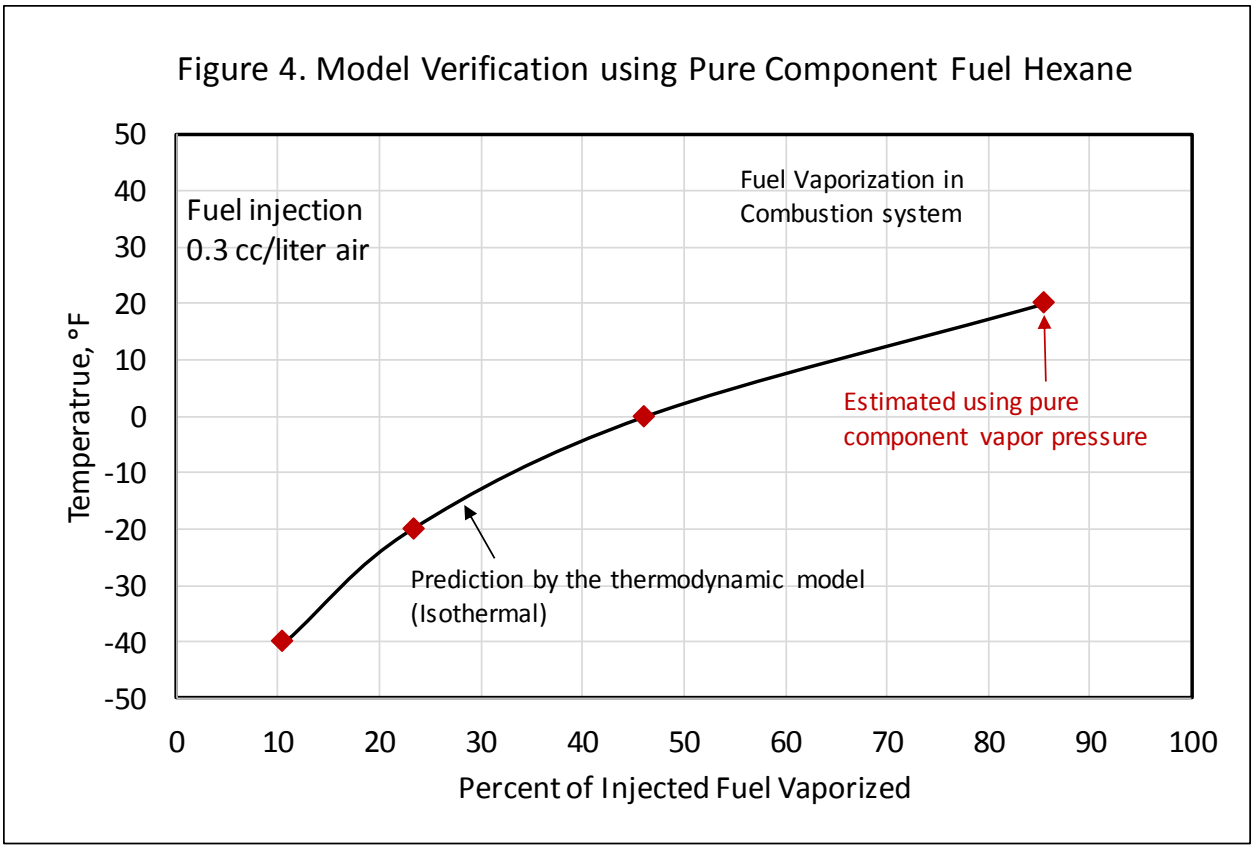

Table 1
Comparison of Model Predicted HOV (KJ/Kg) and Charge Cooling with NREL Data

	Thermodynamic Model		NREL Data/Calculations	
Fuel Blend	HOV, KJ/Kg	Charge Cooling,°F	HOV, KJ/Kg	Charge Cooling,°F
Base Fuel	375	-36	360	-35
Base + 10%EtOH)	433	-43	425	-42
Base + 20%EtOH)	490	-49	485	-49

Thermodynamic Model vs. ASTM Distillation Temperatures

Cold-start and warm-up driveability problems arise if the amount of fuel vaporized is not sufficient for ignition and flame propagation. The thermodynamic model developed in this study predicts vaporization of a given fuel in a cold engine combustion system as a function of temperature and the amount of fuel injected; therefore, the model can be

used to predict driveability problems. The Driveability Index DI_{E0} estimated from ASTM distillation temperatures was found to correlate with vehicle driveability problems [1]; however, the fuel boiling which occurs at high temperatures in ASTM distillation does not simulate partial fuel vaporization in combustion systems at low temperatures. Therefore, the correlation between the ASTM distillation temperatures and driveability may not apply to all fuels. Let us compare ASTM distillation temperatures and model predicted fuel vaporization at low temperatures for various fuels including ethanol-containing fuels. Figure 5 shows ASTM distillation temperatures of two hydrocarbon fuels with different DI_{E0} values and model predicted fuel vapor vaporization of the same fuels for injection of 0.2 cc fuel/liter air (A/F=8.7) at various temperatures.

Figure 5. Comparison of ASTM Distillation and Predicted Fuel Vaporization in Combustion System of two Hydrocarbon Fuels (CRC-666 Fuels: B0 and H3)

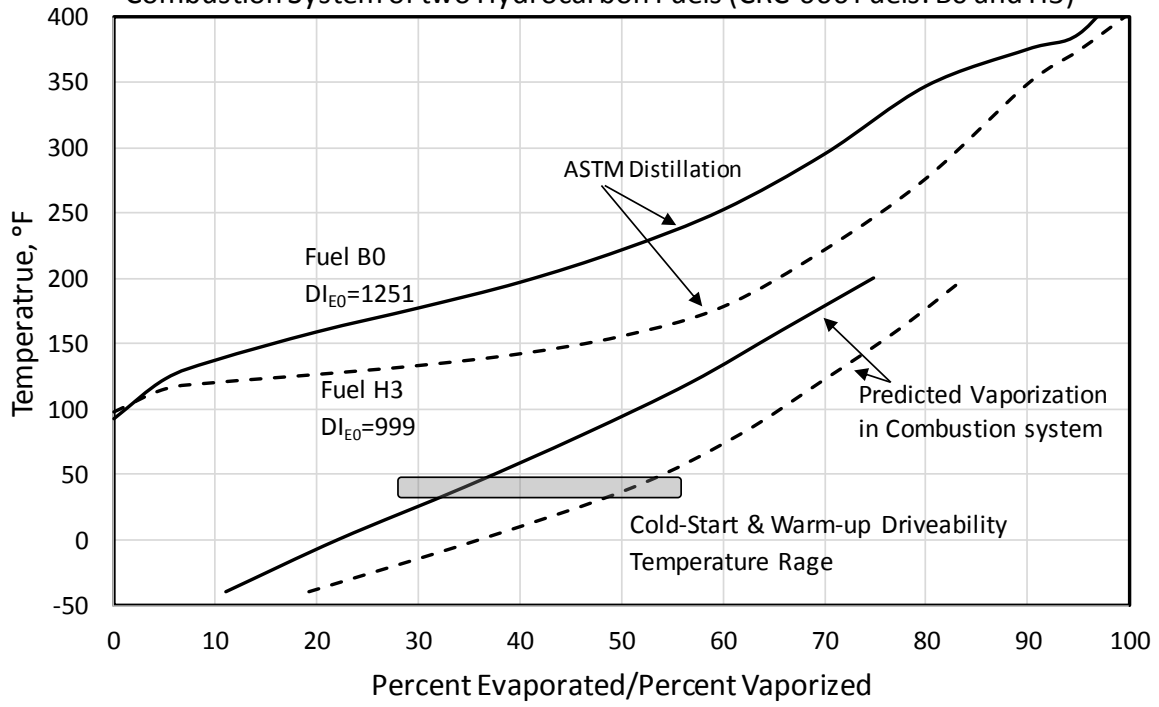

The ASTM distillation temperatures indicate that fuel H3 with a relatively low DI_{E0} of 999 will have better driveability than fuel B0, and CRC-666 data showed the same. The average total weighted demerits (TWD) with fuel H3 were 19 compared to 31 in the case of fuel B0 [3]. The thermodynamic model also shows a similar trend, i.e., better vaporization of fuel H3 compared to fuel B0 (e.g., at 40°F, 51% of fuel H3 vaporizes

compared to only 35% in the case of fuel B0). Therefore, ASTM distillation temperatures and the model predicted fuel vaporizations agree in the estimation of fuel performance for cold-start and warm-up driveability. Now let us perform a similar comparison using a hydrocarbon fuel and an ethanol-containing fuel as shown in Figure 6.

Figure 6. Comparison of ASTM Distillation and Fuel Vaporization in Combustion System of a Hydrocarbon Fuel and an Ethanol Containing Fuel (CRC-666 Fuels: B0 and B2)

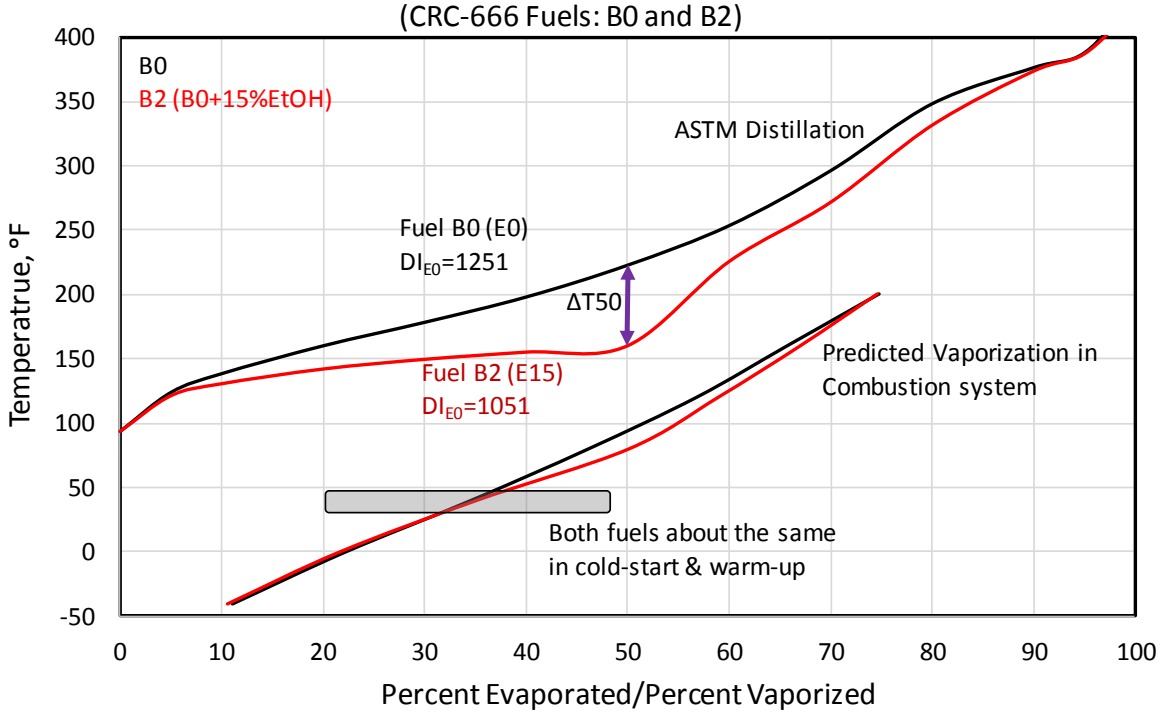

Figure 6 shows the comparison E0 fuel (hydrocarbon fuel B0) and E15 blend (fuel B2). Addition of 15% ethanol to fuel B0, resulted in the depression of T50 and a significant decrease in DI_{E0}. Hence, the ASTM distillation temperatures and DI_{E0} indicate that the driveability performance will be better with fuel B2 (E15 blend). However, the vehicle data show that the TWD were nearly the same (31 and 28 with fuels B0 and B2, respectively). The thermodynamic model shows that vaporization of both the fuels is about the same (e.g., 35% vaporization at 40°F) in the temperature range of interest (35-45°F). Therefore, the T50 depression of the E15 blend (fuel B2) is a misleading indicator of fuel driveability performance which suggests that T50 depression by ethanol should be eliminated or corrected from the DI estimation as shown below:

$$DI_{\Delta T50} = 1.5*T10 + 3.0*T50 + T90 + 3.0*\Delta T50 \quad (8)$$

where $DI_{\Delta T50}$ is the revised driveability Index, ΔT50 is the T50 depression caused by ethanol in gasoline as shown in Figure 6 (i.e., $\Delta T50 = T50_{BOB} - T50_{Blend}$). The revised driveability index $DI_{\Delta T50}$ of the E15 blend was 1237 comparing well with fuel B0 in driveability performance.

Figure 7 shows ASTM distillation temperatures and predicted fuel vaporizations of all four fuels containing different amounts of ethanol. Once again, the thermodynamic model predicted fuel vaporization in a cold engine combustion system show no significant difference in the four fuels contrary to the ASTM distillation temperature results.

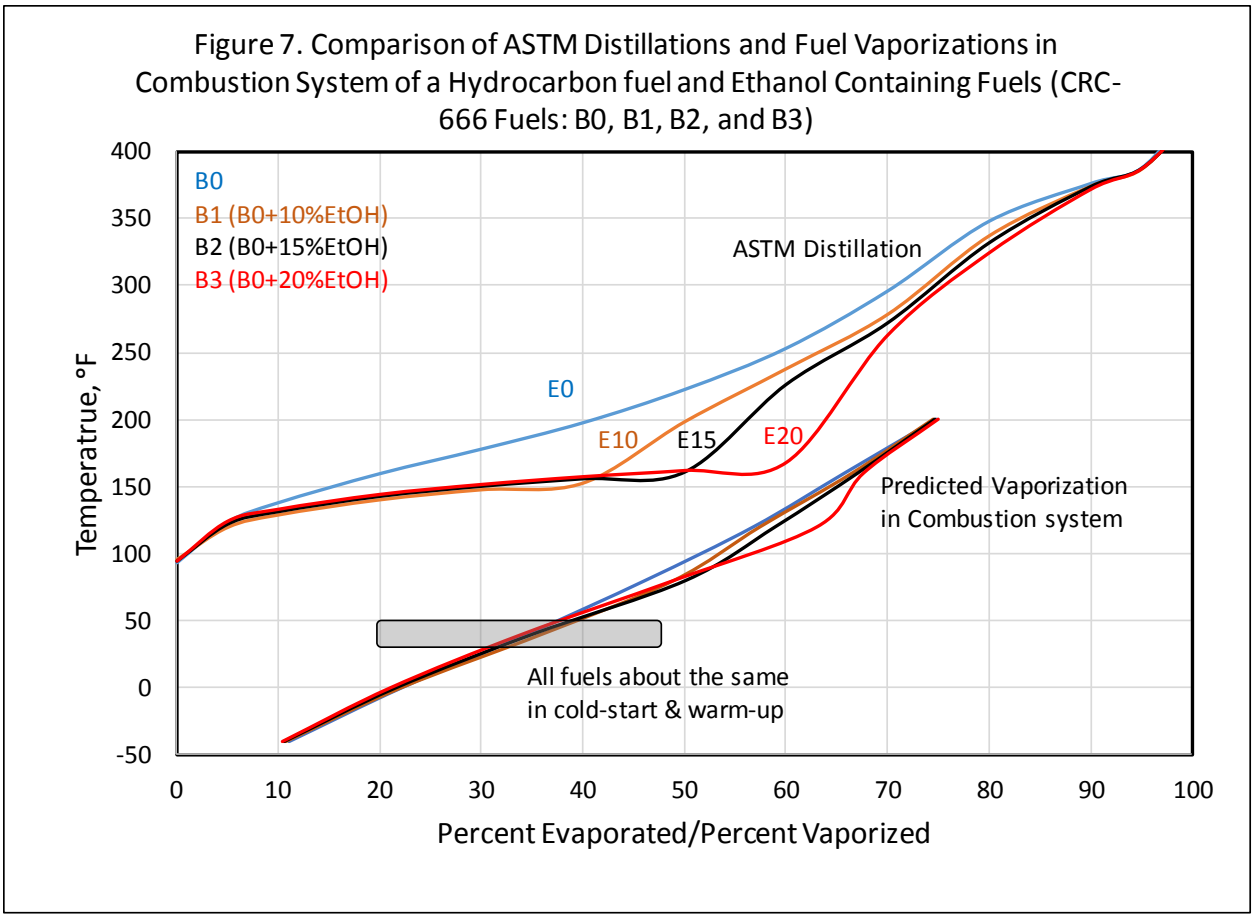

Figure 7. Comparison of ASTM Distillations and Fuel Vaporizations in Combustion System of a Hydrocarbon fuel and Ethanol Containing Fuels (CRC-666 Fuels: B0, B1, B2, and B3)

Figure 8 shows ASTM D86 distillation temperatures and predicted fuel vaporization in a cold combustion system with the all-hydrocarbon fuels used in the CRC-666 driveability study. Both ASTM distillation temperatures and fuel vaporization calculations show the same trend which is fuel H3 is better than fuel H2, which is better than fuel H1 for driveability, and driveability data agrees as discussed below.

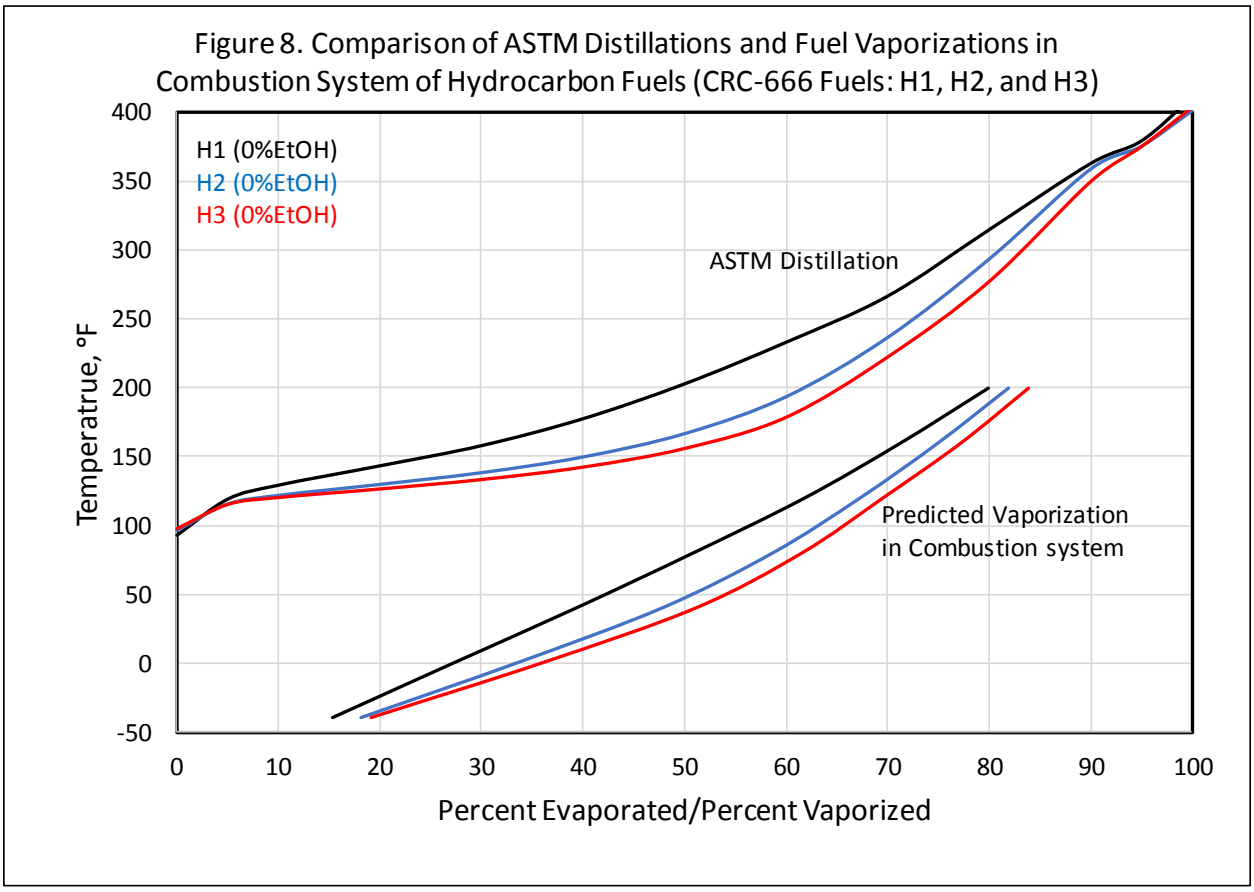

Figure 9 shows the ASTM distillation temperatures and predicted fuel vaporizations of the fuels used in the CRC-638 driveability study. The figure shows that the predicted fuel vaporization was nearly the same in all cases. However, there was no significant T50 depression unlike the case of the CRC-666 fuels because of the low concentration of ethanol; as a result, the DI_{E0}s of the four fuels were nearly the same, and, also, the driveability performances were nearly the same [2]. Therefore, the CRC-638 data were not useful for the purposes of this study, and it is not discussed further in this report.

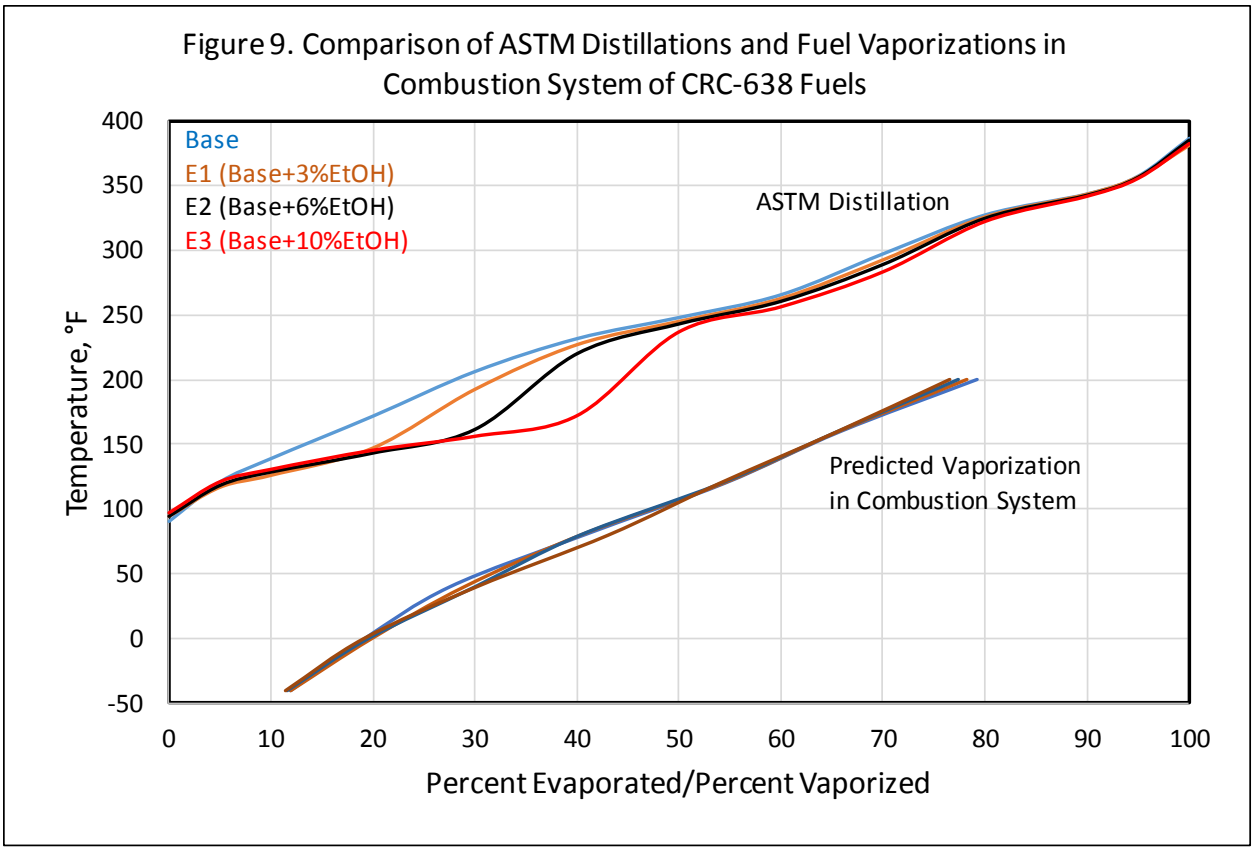

To understand the discrepancy between ASTM distillation temperatures and predicted fuel vaporizations, ethanol effects (i.e., positive effect of vapor pressure increase and negative effect of charge cooling) were separated as shown in Figure 10. ASTM distillation temperatures and predicted fuel vaporizations agree when charge cooling is ignored (see Figure 10) which indicates that ASTM distillation temperatures do not capture the charge cooling effect of fuel vaporization in a cold engine combustion system.

Table 2 shows both the uncorrected DI (DI_{E0}), corrected DI (DI_{E20}) and revised DI ($DI_{\Delta T50}$) of the CRC-666 fuels shown in Figures 7 and 8. As explained in the CRC-666 report, the driveability data (TWD) was log transformed for correlating with fuel driveability index [3]. It was not possible to include the other three CRC-666 oxygenated fuels (B4, B5, and B6) because their T50 depressions were not available. They will be included in the second part of this study to develop a method for estimating the T50 depression of ethanol blends.

Figure 10. Illustration of Positive Effect of Ethanol on Fuel Vapor Pressure increase with CRC-666 Fuels (Ignoring Negative Effect of Ethanol on Charge Cooling or HOV=0)

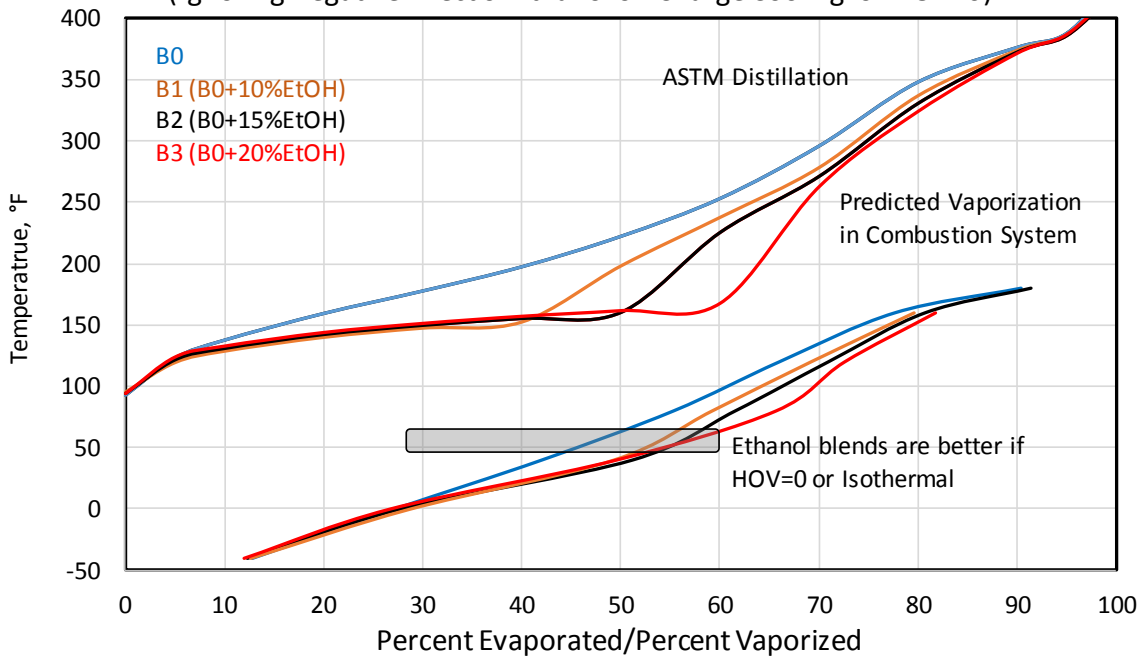

Table 2

Driveability Indexes and Driveability Demerits Data of CRC-666 Fuels

Fuel	DI_{E0}	DI_{E20}	$\Delta T50$	$DI_{\Delta T50}$	Ln TWD
B0	1251	1251	0.0	1251	3.44
B1	1161	1258	24.4	1234	3.36
B2	1151	1200	62.1	1237	3.33
B3	1055	1255	60.9	1238	3.40
H1	1164	1164	0.0	1164	3.12
H2	1042	1042	0.0	1042	2.93
H3	999	999	0.0	999	2.93

The correlation between DI_{E0} and Ln TWD (columns 2 and 6 in Table 2) of the seven fuels shown above, was very poor (R^2=0.3288) because of the misleading T50 depression of ethanol-containing fuels. Figure 11 shows an excellent correlation between revised driveability index $DI_{\Delta T50}$ and Ln TWD (R^2=0.9398). The correlation between DI_{E20} (ethanol corrected DI) and Ln TWD (columns 3 and 6 in Table 2) of the seven fuels shown above, was (R^2=0.9348). The next phase of this study will focus on development of a model for estimating the T50 depression of any gasoline-ethanol blends to compute $DI_{\Delta T50}$.

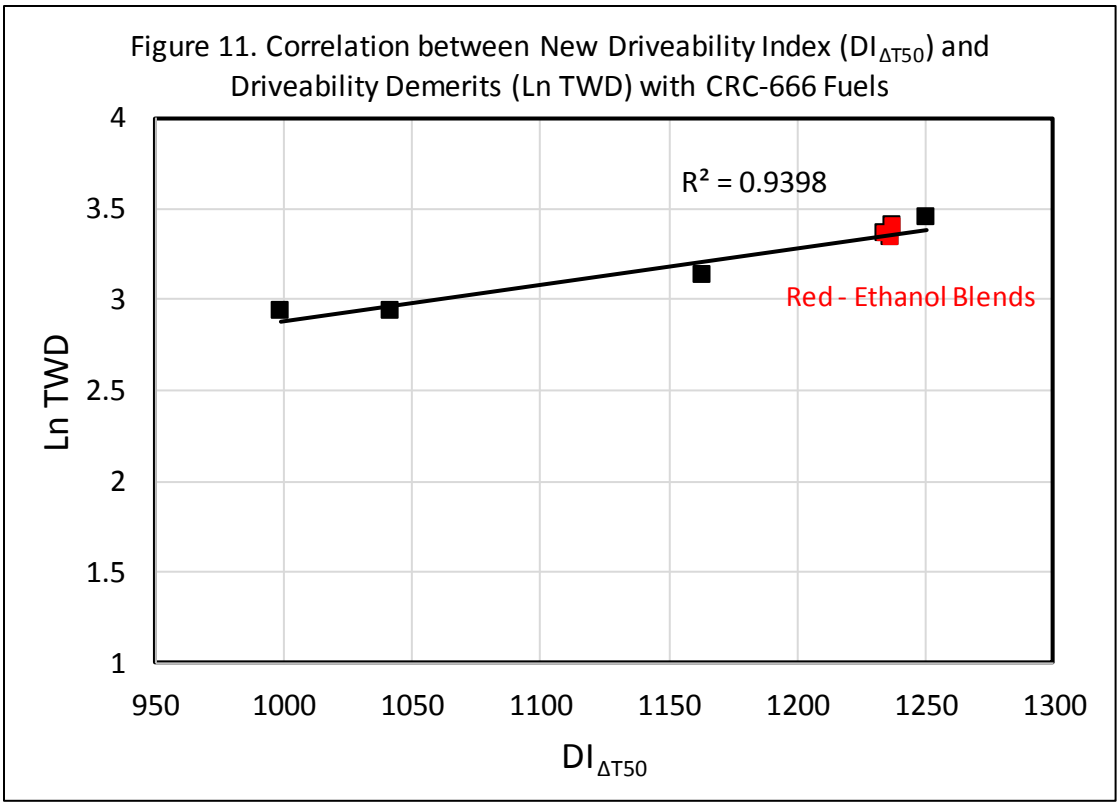

Estimation of T50 Depression (ΔT50) of Gasoline-ethanol Blends for Computing $DI_{\Delta T50}$

For estimating the revised driveability index ($DI_{\Delta T50}$) of a gasoline-ethanol blend, we need to determine ΔT50 of the blend. It will be very simple to determine ΔT50 if the T50 of the base fuel or BOB is available ($\Delta T50 = T50_{BOB} - T50_{blend}$). However, $T50_{BOB}$ is not available in most cases. Therefore, we have to estimate the ΔT50 of an ethanol blend from commonly measured blend properties such as vol % ethanol, ASTM distillation temperatures, DVPE, etc. Figure 12 shows the problem with what we are trying to accomplish, which is the prediction of T50 depression without knowing the base fuel T50.

A thorough analysis of ASTM distillation temperatures of a variety of gasoline-ethanol blends was conducted to develop equations for estimating T50 depression as a function of blend distillation temperatures and ethanol concentration. There were two excellent

Figure 12. Illustration of the Problem in the Estimation of ΔT50 without knowing T50 of Base Fuels

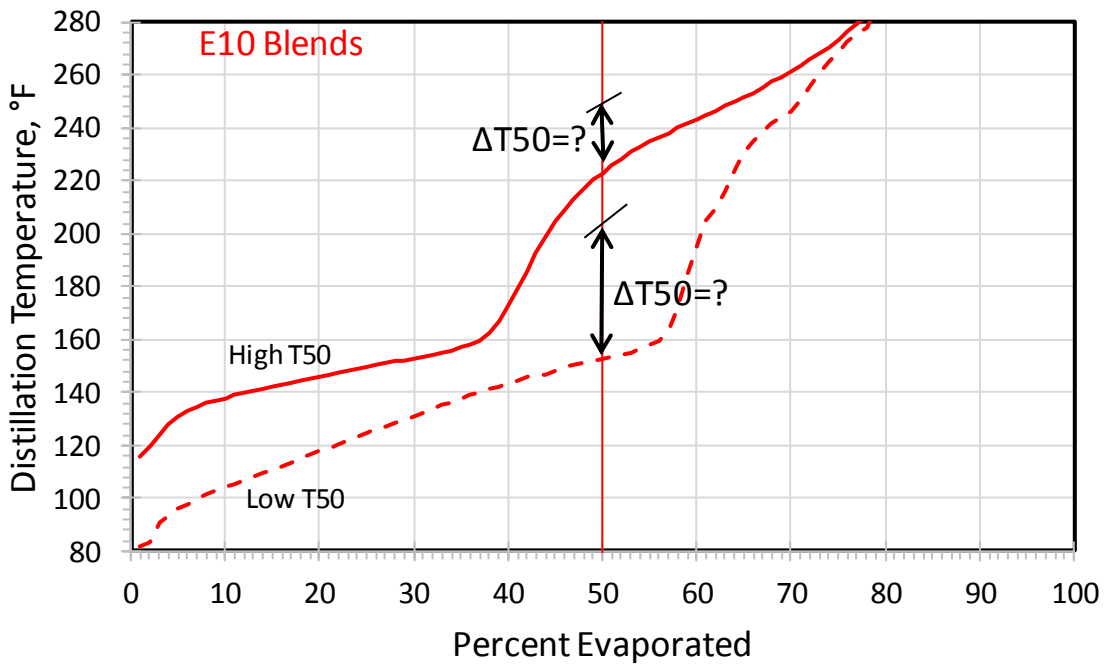

sources of data available for this study [16,17]. An API study [16] consisted of 71 base stocks for ethanol blending (55 commercial ethanol-free fuels + 13 BOBs (Blend stocks for Oxygenate Blending) + 3 CRC-658 low T50 test fuels). These fuels were splash blended with 10, 12.5, 15, 20 and 30 vol % denatured ethanol. In further discussion, base fuel refers to both base stock and BOB. The distillation data was incomplete for two fuels and the distillation data of another three fuels (CRC-658 low T50 test fuels) were outliers in some of the analyses. The CONCAWE/SHELL study [17] also known as the BEP525 Ethanol/Petrol Blending Study, a statistically designed experimental program covering a wide range of fuel volatilities and compositions, consisted of 60 specially formulated base stocks splash blended with 5, 10, 15, 20, 25 vol % denatured ethanol. In the CONCAWE/SHELL study, each fuel blend was tested in triplicate and the averages of the triplicate test data were used in all of the present analysis.

The first step in the data analysis was computing average T50 depression (ΔT50avg) as a function of ethanol concentration. The averages were computed separately for the API and the CONCAWE data, and the results are shown in Figure 13. These results

show a non-linear trendline that can be described by a Sigmoid mathematical function ("S" shape) which is represented by the following well known mathematical equation:

$$\Delta T50_{avg} = \frac{A}{1+B.e^{-C.EtOH}} \quad (9)$$

where A, B, and C are constants, and EtOH is the ethanol concentration (vol %) in the fuel blend. The non-linear curve fitting optimization option in MS Office Excel® was used to compute the best values for A, B, and C for both data sets which are shown in Figure 13. Since the API data did not include any blends with 5% ethanol (E5), the CONCAWE E5 blends average T50 depression was used for curve fitting the API data.

Figure 13. Average T50 Depression (ΔTavg) as a Function Ethanol Concentration

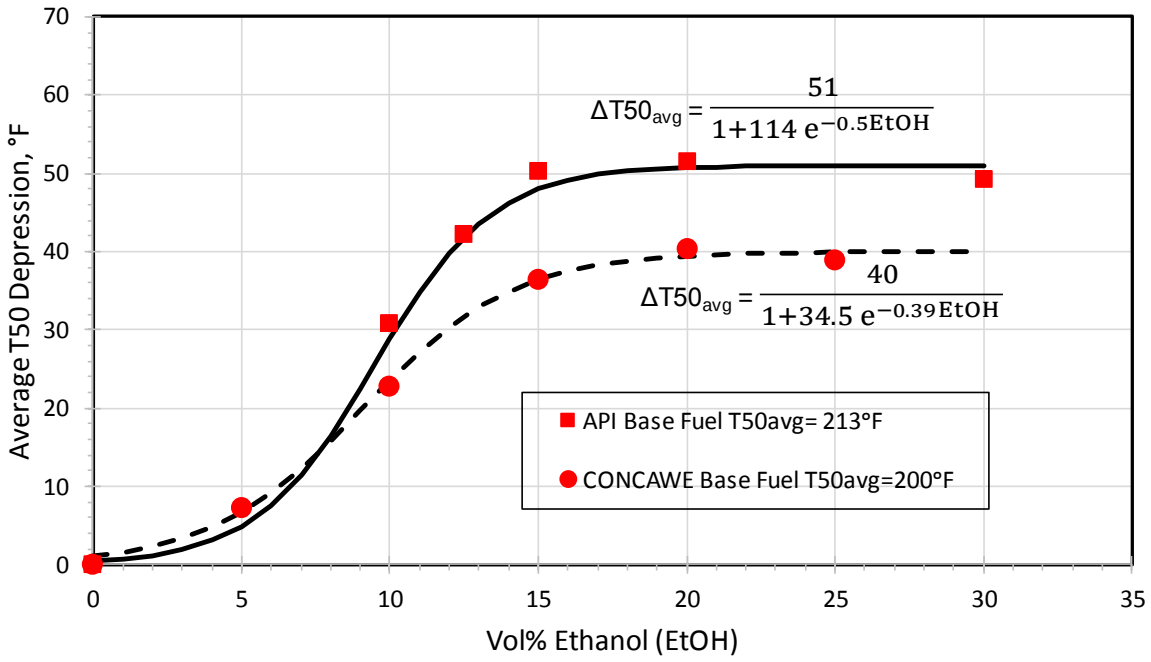

Note that the average T50 depressions were lower for the CONCAWE ethanol blends compared to the API ethanol blends (e.g., 10°F lower T50 depression observed for the CONCAWE E20 blends). The main reason for this observation appears to be the lower T50s of the CONCAWE base stocks (as shown in Figure 13, the $T50_{avg}$ of the CONCAWE base fuels was 13°F lower than that of the API base fuels). Since API base stocks were more representative of US fuels than CONCAWE base stocks, the API

dataset was used for developing equations for estimating the T50 depression of ethanol blends.

CRC-666 driveability data was re-plotted in Figure 14 by estimating $DI_{\Delta T50}$ using the equation $\Delta T50=\Delta T50_{avg}$ as shown below:

$$DI_{\Delta T50} = 1.5*T10 + 3.0*T50 + T90 + 3.0*(51/(1+114*e^{-0.5*EtOH})) \quad (10)$$

Note that the last term in Equation (10) becomes negligible if EtOH = 0 (i.e., $\Delta T50_{avg}$= 0.4 when EtOH = 0). Therefore, Equation (10) is applicable to both hydrocarbon fuels and ethanol blends. The correlation in Figure 14 includes three additional CRC-666 fuel blends B4, B5, and B6 that were not included in the correlation shown in Figure 11. If the three additional fuels (B4, B5, and B6) are not included, the correlation coefficient is $R^2 = 0.9068$, compared to $R^2 = 0.9398$ when actual measured values of T50 depressions were used (Figure 11). It is reasonable to expect a slight deterioration in correlation coefficient when $\Delta T50_{avg}$ is used instead of measured ΔT50 ($R^2 = 0.9068$ with $\Delta T50 = \Delta T50_{avg}$ vs. $R^2 = 0.9398$ with measured ΔT50).

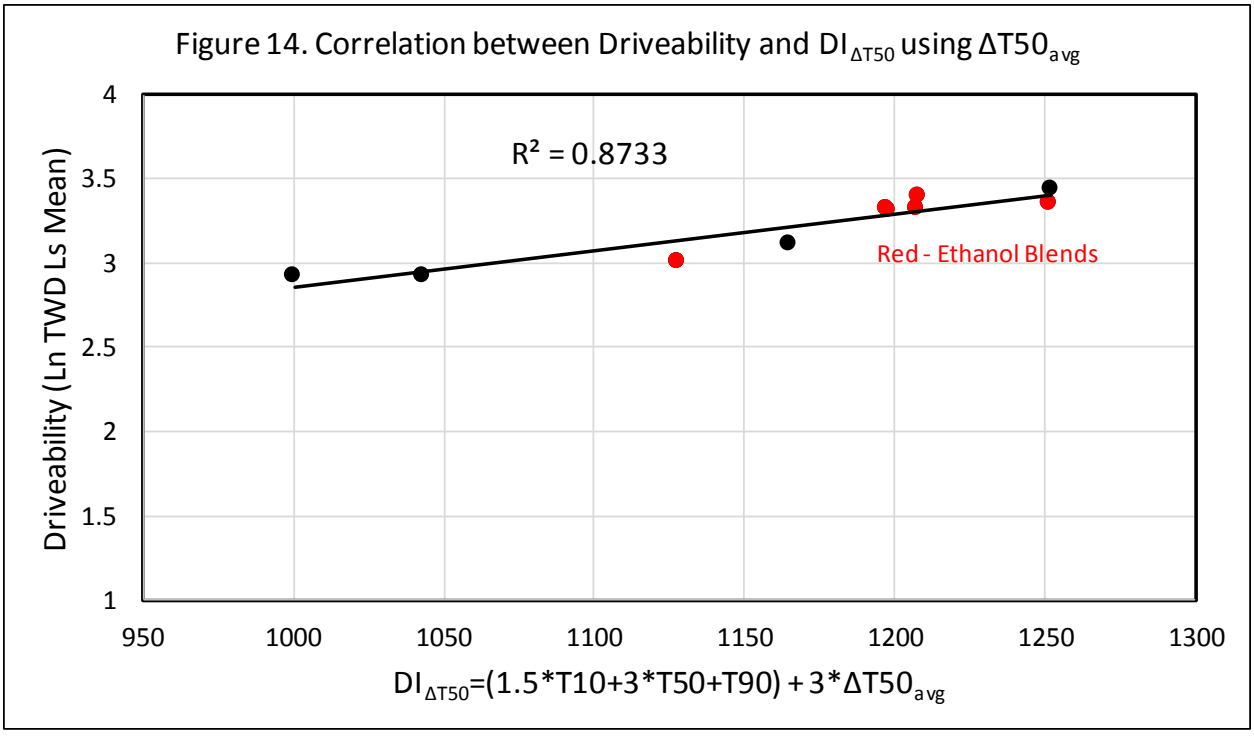

The revised driveability index $DI_{\Delta T50}$ using $\Delta T50_{avg}$ (Equation (10)) correlates very well with CRC-666 data; however, as seen in Figure 15, the data shows wide variations in ΔT50 for any given ethanol concentration. For example, $\Delta T50_{avg}$ of E15 blends is 48°F but the measured ΔT50 of those E15 blends varied from 22 to 65°F. The next step is to understand why some E15 blends have low ΔT50 and some other E15 blends have high ΔT50. Such understanding should lead to more accurate estimations of ΔT50 by using other properties of ethanol blends in addition to ethanol concentration.

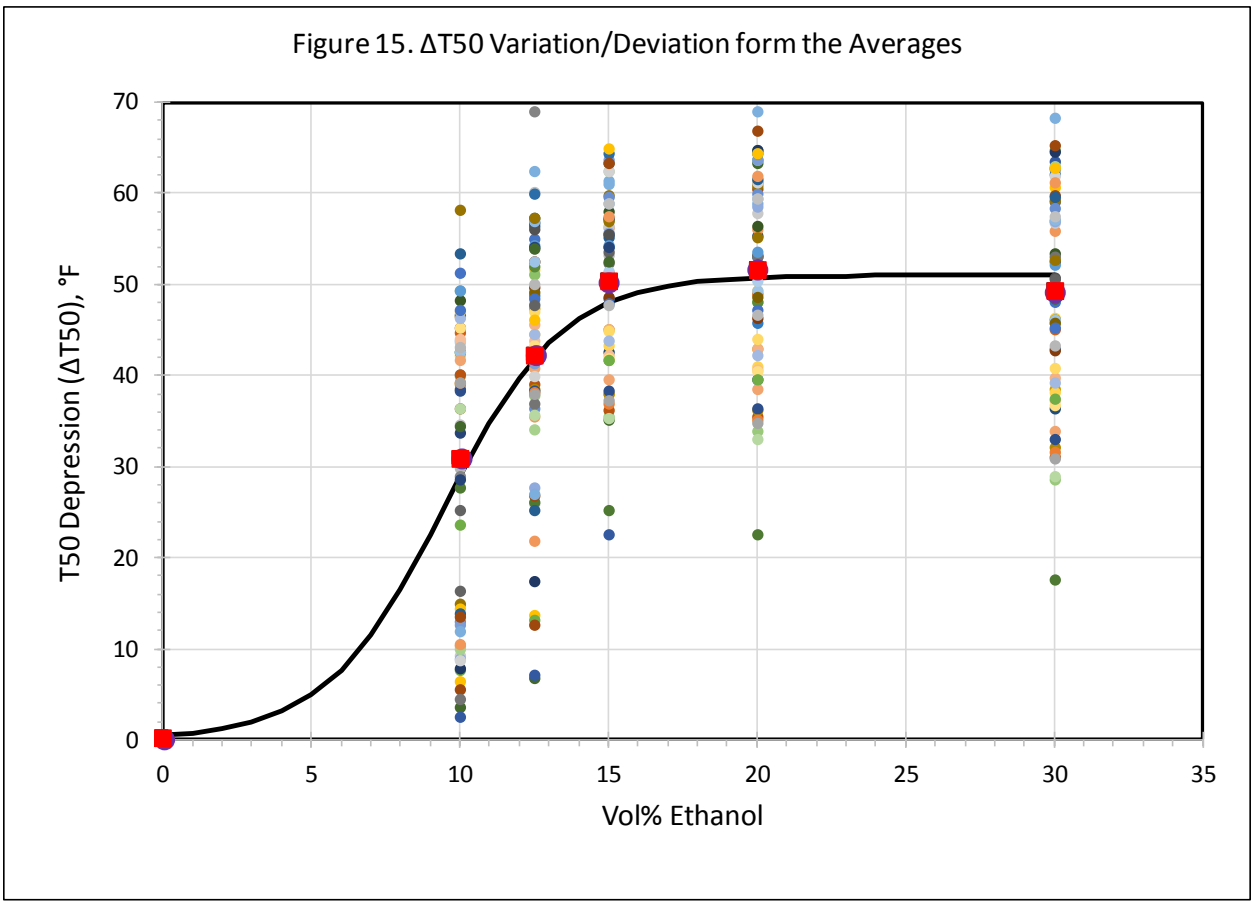

Further analysis of API data [16] was conducted to determine what causes wide variations in ΔT50 for a given ethanol concentration and how to predict deviations from $\Delta T50_{avg}$ from known properties such as ASTM distillation temperatures. Figure 16 shows T50 depressions (ΔT50) of all the API ethanol blends as a function of base fuel T50. The results show the following trends:

1. Little or no T50 depression occurs if the base fuel T50 is low (<150°F).

2. In most cases, ΔT50 increases with base fuel T50, except in the case of E10 and E12.5 blends whose ΔT50 increases with base fuel T50 up to T50=205°F, and thereafter ΔT50 decreases with increasing base fuel T50. The reason for little or no T50 depression of high T50 base fuels is that distillation temperature depression (T depression) occurs before T50, as observed in Figures 7 and 9.
3. Excellent correlation (R^2=0.995) exists between ΔT50 of E20 and E30 blends and base fuel T50 because of the temperature depression of E20 and E30 blends always occurs at base fuel T50. Unfortunately, these correlations are not useful because we assume that the base fuel T50 is not available for estimating the ΔT50 of a blend (only the blend T50 is available).

Figure 16. T50 Depression of Ethanol Blends as a Function of Base Fuel T50

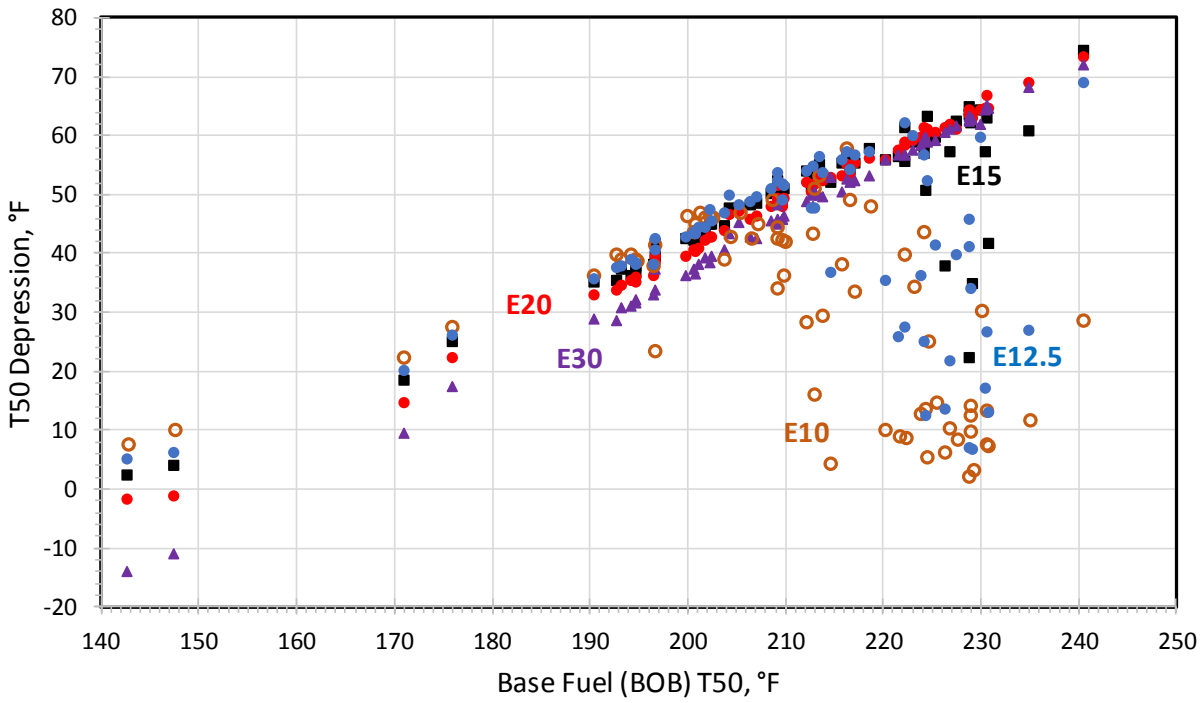

However, there is a need to develop equations for estimating the ΔT50 of ethanol blends using blend properties, not base fuel properties. Analyses were conducted to determine what properties of an ethanol blend correlate well with its T50 depression. Correlations were studied between ΔT50 and blend DVPE, T10, T40, T50, and T50-

T_{BP_EtOH} (T_{BP_EtOH} is the boiling point temperature of ethanol which is 173°F). Correlation between ΔT50 and blend T50 was the best option, as discussed in detail in the following sections.

Based on the data analysis, the following equation is proposed for ΔT50:

$$\Delta T50 = F * \Delta T50_{avg} \quad (11)$$

where F is a correction factor, and it was found to be a function of blend properties including distillation temperatures and ethanol concentration.

$$F = f(\text{Blend DVPE, Distillation Temperatures, EtOH, etc.}) \quad (12)$$

Again attempts were made to find a correlation between F and DVPE, T10, T40, T50, T50-T_{BP_EtOH}, and EtOH. However, the most useful correlation was found between F and blend T50 alone as presented below, because it yielded better results, and it is simpler to use for ΔT50 estimation.

Note that attempts were also made to develop an alternate equation for ΔT50 which is shown below:

$$\Delta T50 = \Delta T50_{avg} + \Delta T50_{Deviation} \quad (13)$$

where $\Delta T50_{Deviation}$ is a correction to average $\Delta T50_{avg}$, that is deviation from $\Delta T50_{avg}$. Reasonably good correlations were found between $\Delta T50_{Deviation}$ and EtOH and blend T50 for some of the blends. The correlation between $\Delta T50_{Deviation}$ and blend T50 & EtOH or $\Delta T50_{Deviation} = f$(Blend T50, EtOH) is developed in Appendix C.

Equation (11) can be written as:

$$\Delta T50 = F * \frac{51}{1+114\ e^{-0.5\ EtOH}} \quad (14)$$

Note that the form of Equation (14) makes it very convenient to modify as needed. If a simple equation is desired for an approximate estimation of T50 depression, ignore the

correction factor (F = 1). On the other hand, if a more accurate estimation is required, use both terms in Equation (14).

API data was used to compute the correction factor F ($F = \text{Measured } \Delta T50 / \Delta T50_{avg}$) and plotted as a function of blend T50 as shown in Figure 17. An inverted parabola (MS Office Excel® 2-order polynomial) was the best trendline for the data (dotted line in Figure 17); however, the trendline equation ($F = -0.0006 (T50 - 176)^2 + 1.2$) becomes invalid (i.e., F becomes a meaningless large negative number) for blends with very low T50 (T50 < 130°F) and also for blends with very high T50 (T50 > 225°F). To over comes this problem, a bell shaped curve was selected for the trendline. The bell curve equation contains three constants ($F = A\ EXP(-(B*T50 - C)^2)$) and they were estimated by using non-linear curve fitting optimization option in MS Office Excel®, which resulted in the following equation:

$$F = 1.2\ e^{-(0.029*T50\ -5)^2} \tag{15}$$

Combining Equations (14) and (15) results:

$$\Delta T50 = \left(1.2\ e^{-(0.029*T50\ -5)^2}\right)*\left(\frac{51}{1+114\ e^{-0.5*EtOH}}\right) \tag{16}$$

In MS Office Excel®, Equation (16) appear as follows:

$$\Delta T50 = (1.2*EXP(-((0.029*T50-5)^2)))*(51/(1+114*EXP(-0.5*EtOH))) \tag{17}$$

If T50=190 and EtOH=10, computed value of ΔT50 should be 26.7

Note that Equation (16) is valid for all ethanol blends (including E0) with any T50. If a blend T50 is low (T50 < 130°F), $F \rightarrow 0$ and the same is true if a blend T50 is high (T50 > 225°F). In both cases, as expected $\Delta T50 \rightarrow 0$. Figure 18 shows two examples, a high T50 blend and a low T50 blend, for which ΔT50 is nearly zero. Therefore, the correction F (the first term in Equation (16)) makes the equation to be valid for any T50.

Figure 17. Correction Factor F ($F = \Delta T50/\Delta T50_{avg}$) as a Function of Blend T50

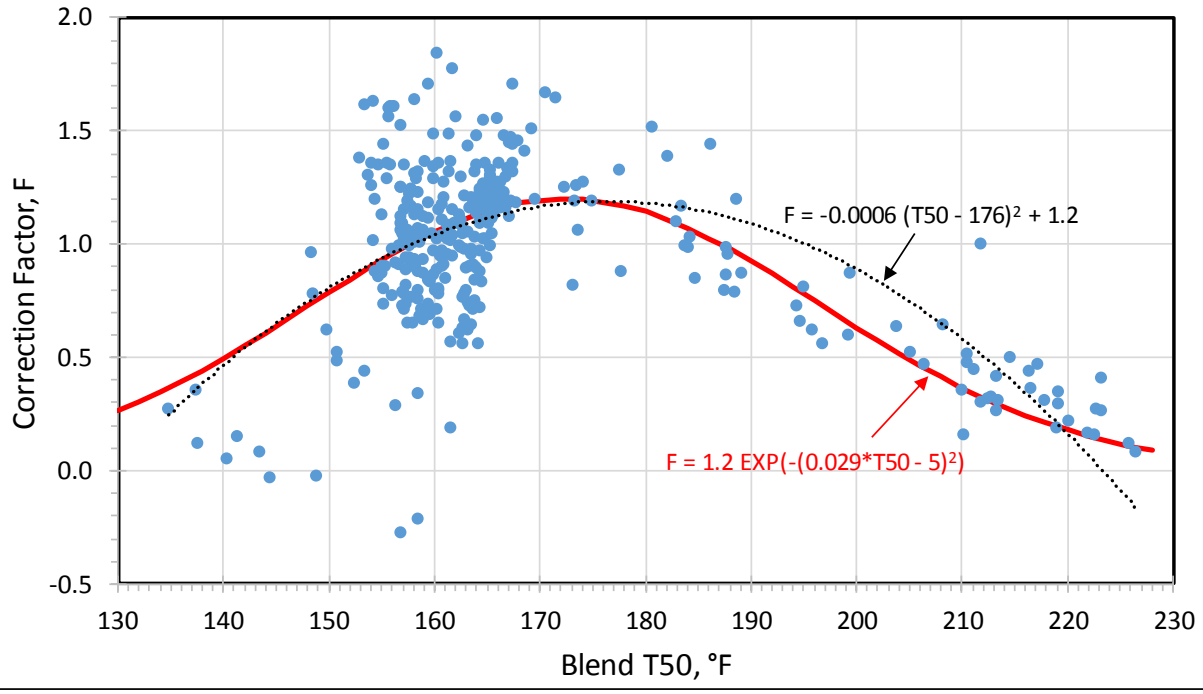

Figure 18. Examples of High and Low T50 Blends with ΔT50 = 0.

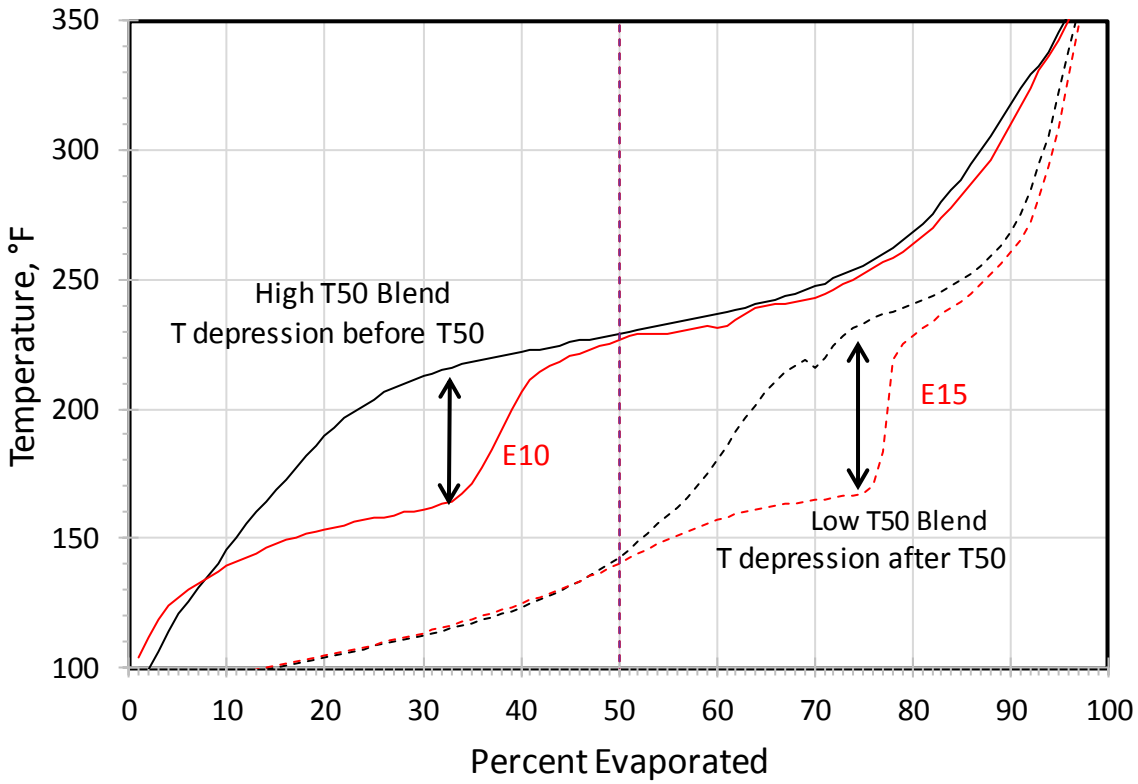

API data was used to determine correlation between measured T50 depression ($\Delta T50_{Measured}$) and T50 depression predicted ($\Delta T50_{Predicted}$) by Equation (16) and the results are shown in Figure 19. Note that the correlation was much better for E10 – E15 blends (R^2 = 0.7202) than it was for all the blends (R^2 = 0.3954). The reason for the better correlation for E10 - E15 blends is that the bell curve in Figure 17 was a better representation of the trends of E10-E15 blends than it was for E20 and E30.

Figure 19. Correlation Between Measured and Predicted ΔT50

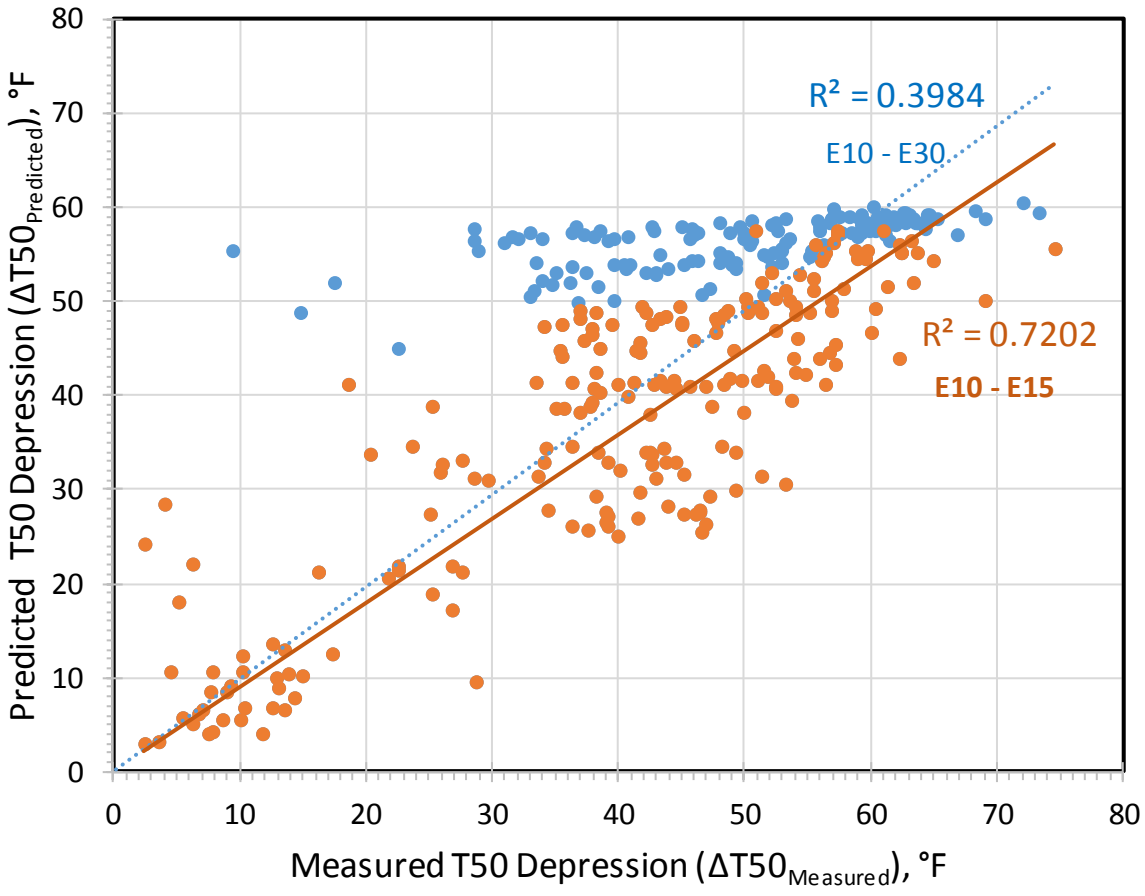

CRC-666 driveability data was re-analyzed by re-computing $DI_{\Delta T50}$ using Equation (16) for ΔT50 estimation, and the results are shown in Figure 20. The correlation between $DI_{\Delta T50}$ and driveability performance was about the same (R^2=0.8733 in Figure 14) when $\Delta T50=\Delta T50_{avg}$ was used, compared to the correlation when $\Delta T50=F*\Delta T50_{avg}$ was used (R^2=0.8691 in Figure 20). The reason for no change in the correlation is that the value

of F is nearly equal to 1 for CRC-666 fuels because of their T50 values correspond to F=1 in Figure 17.

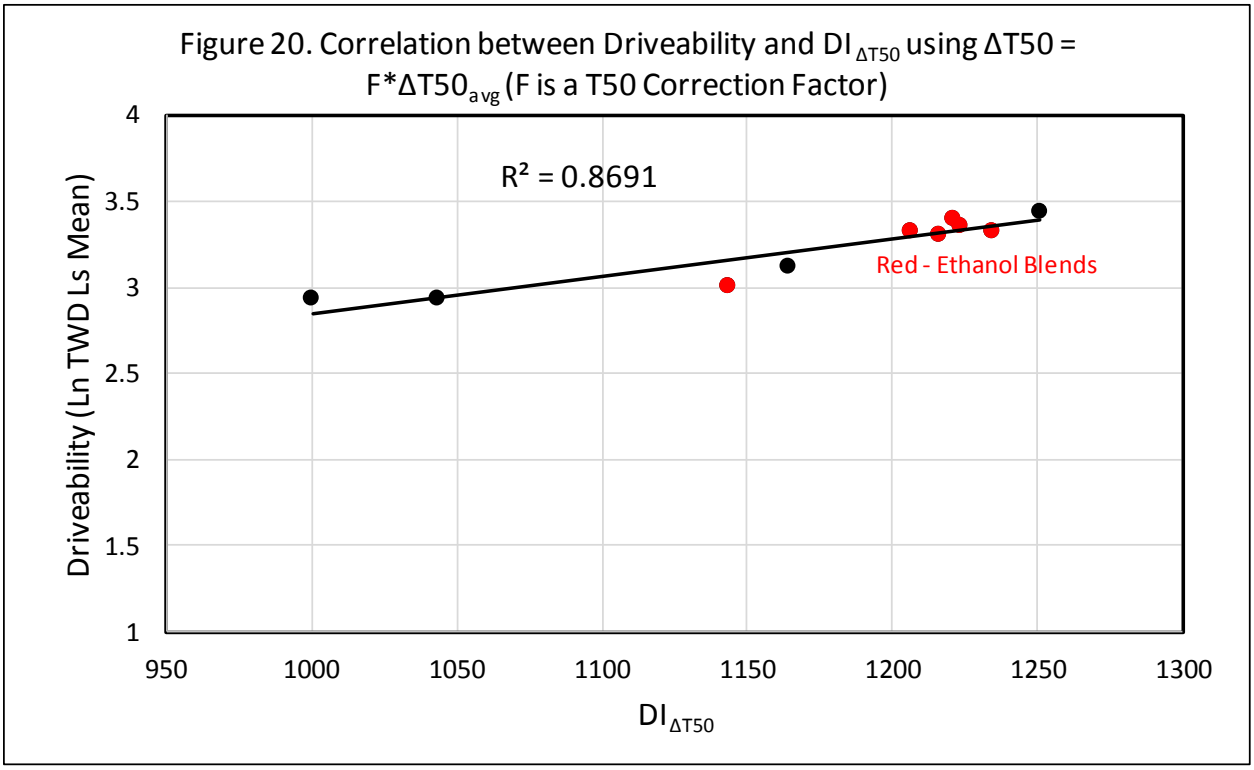

In search of an improved method for estimating revised driveability index $DI_{\Delta T50}$, it was decided to conduct data analysis to develop the following relationship applying the ΔT50 correction to the DI equation.

$$DI_{\Delta T50} = DI_{E0\_BOB} = f(DI_{E0\_Blend}) \quad (18)$$

Where DI_{E0_BOB} is uncorrected DI of the base fuel, which is not known but is expected to be a function of uncorrected DI of the blend DI_{E0_Blend}. API data were used to compute DI_{E0_Blend} of various blends and determine a correlation equation between DI_{E0_Blend} and DI_{E0_BOB}, which can then be used to estimate $DI_{\Delta T50}$. Appendix D shows the detailed analysis of this method of $DI_{\Delta T50}$ estimation. The analysis found that DI_{E0_BOB} correlates with DI_{E0_Blend}; however, it was not possible to develop a single equation applicable to all ethanol blends as discussed in Appendix D.

Summary

Vehicle cold-start and warm-up driveability performance of hydrocarbon fuels correlates inversely with the fuel driveability index (DI), which is estimated from ASTM D86 distillation temperatures (DI= 1.5*T10+3*T50+T90). Blending ethanol (up to 20%) with gasoline decreases DI by depressing T50, which implies better driveability with gasoline-ethanol blends; however, the test data show little or no driveability improvement. Based on CRC studies, empirical ethanol correction factors were added to the DI equation without understanding the mechanism of the ethanol effect on ASTM distillation temperatures and vehicle driveability.

To understand the effect of ethanol, a thermodynamic model was developed for predicting fuel vaporization in cold combustion systems as a function of ethanol concentration in the fuel. The model showed that the T50 depression (ΔT50) by ethanol is a misleading indicator of driveability improvement; therefore, a modified driveability index $DI_{\Delta T50}$ is proposed ($DI_{\Delta T50}$=1.5*T10+3*T50+T90+ 3*ΔT50), which correlates well with CRC-666 driveability data. For a given ethanol blend, T10, T50, and T90 are available from fuel inspection data; however, the challenge was the estimation of ΔT50 without knowing base fuel or BOB T50.

API data was used to develop equations for estimating ΔT50 as shown below:

$$\Delta T50 = F*\Delta T50_{avg}$$

where $\Delta T50_{avg}$ is average T50 depression as a function of ethanol concentration and F is correction factor for the variations in blend T50. The equations were developed for F and $\Delta T50_{avg}$ as shown below:

$$\Delta T50 = \left(1.2\, e^{-(0.029*T50\,-5)^2}\right)*\left(\frac{51}{1+114\, e^{-0.5*EtOH}}\right)$$

Whenever a simple equation is desired for approximate estimation, especially for E15-E30 blends, $DI_{\Delta T50}$ can be estimated using only the second term in the equation (i.e.,

$\Delta T50 = \Delta T50_{avg}$). If a more accurate estimation of ΔT50 is desired, especially for E10 blends, both terms in the equation should be used.

Acknowledgements

Thanks to Bill Cannella of Chevron for providing detailed hydrocarbon analysis of CRC-638 and CRC-666 fuels, which was essential for the first part of the study. Thanks to David Lax of API for providing the data of mid-level ethanol blends, which was essential for the second part of the study. Thanks to Ken Rose of ExxonMobil for providing some useful information and a reference for CONCAWE data file. The CRC Volatility Group (panel members shown below) guidance and support is greatly appreciated.

Jim Simnick (Panel Leader)	BP
Bill Cannella	Chevron
John Cruz	Daimler
Lewis Gibbs	Consultant
Steve Vander Griend	ICM
Gary Herwick	Consultant
David Lax	API
Michael Lynch	ExxonMobil
Rebecca Monroe	Fiat Chrysler
Christopher Pritchard	FHR
Daniel Short	Marathon
Jenny Sigelko	VW
Bill Studzinski	GM
Mark Winston Galant	GM

References

1. D. A. Barker, L. M. Gibbs, and E. D. Steinke, “The Development and Proposed Implementation of the ASTM Driveability Index for Motor Gasolines,” SAE Paper 881668.
2. Coordinating Research Council, Inc., “2003 CRC INTERMEDIATE-TEMPERATURE VOLATILITY PROGRAM,” CRC-638, February 2004.
3. Coordinating Research Council, Inc., “2013 CRC INTERMEDIATE-TEMPERATURE E15 COLD-START AND WARM-UP VEHICLE DRIVEABILITY PROGRAM,” CRC-666, April 2014.
4. CONCAWE, “Volatility and vehicle driveability performance of ethanol/gasoline blends: a literature review,” Report No. 8/09 CONCAWE Brussels, October 2009.
5. S. McArragher, et al., “CONCAWE/GFC Study on Gasoline Volatility and Ethanol Effects on Hot and Cold Weather Driveability of Modern European Vehicles,” SAE Paper 2004-01-2002.
6. C. Colpin, et al., “Key Parameters for Startability Improvement Applied to Ethanol Engines,” SAE Paper 2009-01-0616.
7. P. Geng, et al., “Gasoline Distillation Effect on Vehicle Cold Start Driveability,” SAE Paper 2007-01-4073.
8. R. Bazzani, et al., “The Effects of Driveability on Emissions in European Gasoline Vehicles.” SAE Paper 2000-01-1884.
9. S. R. Reddy, “Evaporative Emissions from Gasolines and Alcohol-Containing Gasolines with Closely Matched Volatilities,” SAE Paper 861556, 1986.
10. S. R. Reddy, “Model for Estimating Vapor Pressures of Commingled Ethanol Fuels,” SAE Paper 2007- 01- 4006, 2007.
11. G. M. Chupka, et al., “Heat of Vaporization Measurements for Ethanol Blends Up to 50 Volume Percent in Several Hydrocarbon Blendstocks and Implications for Knock in SI Engines,” SAE Paper 2015-01-0763.
12. Zabetakis, M.G., “Flammability Characteristics of Combustible Gases and Vapors,” U.S. Bureau of Mines, Bulletin 621, Washington, 1965.

13. R. C. Reid and T. K. Sherwood, Properties of Gases and Liquids, McGraw-Hill, New York, 1966.
14. T. Boublik, V. Fried, and E. Hala, The Vapor Pressures of Pure Substances, Elsevier, New York, 1973.
15. A. Fredenslund, R. L. Jones, and J. M. Prausnitz, “Group-Contribution Estimation of Activity Coefficients in Nonideal Liquid Mixtures,” AIChE Journal, V21, p1086, 1975.
16. American Petroleum Institute, “Determination of the Potential Property Ranges of Mid-Level Ethanol Blends,” Final Report, April 23, 2010.
17. CONCAWE / SHELL RESEARCH, “Ethanol/Petrol Blends: Volatility Characterization in the Range 5-25 Vol %,” Final Report BEP525, December 2009.

Appendix A

Compositions of Fuels used in the Thermodynamic Model

The compositions (GC analysis) of all the fuels used in CRC Projects 638 and 666 were obtained from Chevron Oil Company. The GC analysis consisted of hundreds of different identified and un-identified hydrocarbon compounds. However, there were only about a hundred compounds which were present in appreciable quantities (>0.01%) in the fuels; therefore, only these compounds were considered for representing the fuels. The concentration of the compounds that were not considered were added to the compounds having nearly the same retention time or carbon number. Many of the compounds are isomers of a single compound. Since the UNIFAC theory makes little or no distinction between isomers, some of the low concentration isomers of a compound were added to the predominant isomer. The isomer grouping reduced the number of components significantly. The vapor pressures and other required property data of some of the insignificant compounds were not available; therefore, the compounds for which the data were not available were grouped with the other compounds of nearly the same carbon number. Note that the property data were available for most of the compounds that are present in significant quantities in the fuels. The final list contained eighty-five hydrocarbons that were used to represent fuels in this study. Tables A-1 and A-2 show the compositions of CRC-666 and CRC-638 test fuels, respectively. Note that CRC-666 fuels B1, B2, and B3 were ethanol splash blended fuels of fuel B0, therefore, there was no need to include them in Table A-1 and A-2. Similarly, CRC-638 fuels E1, E2, and E3 were splash blended fuels of the base fuel; therefore, they are not included in Table A-3 and A-4.

Table A-1. Compositions of CRC-666 fuels

CRC 666 Fuel =>	B0	B4	B5	B6	H1	H2	H3
Component	**Wt %**	**Wt %**	**Wt %**	**Wt %**	**Wt %**	**Wt %**	**Wt %**
Propane	0.002	0.004	0.003	0.003	0.007	0.006	0.007
Butane	0.736	0.882	0.992	1.239	0.900	0.642	0.669
Pentane	1.431	1.585	1.739	1.505	1.617	1.206	1.209
Hexane	4.130	2.755	1.548	1.843	3.589	3.675	2.375
Heptane	1.055	1.087	1.220	1.031	1.149	0.849	0.814
Octane	0.439	0.448	0.512	0.428	0.470	0.344	0.335
Nonane	0.187	0.192	0.220	0.184	0.219	0.160	0.155
Decane	0.841	0.315	0.365	0.324	0.366	0.300	0.269
2M-Propane	2.279	0.147	0.152	0.144	0.880	0.474	0.130
2M-Butane	3.601	9.950	8.148	6.815	12.173	13.174	12.838
2,2-DM-propane	0.003	0.005	0.005	0.005	0.006	0.005	0.005
2M-pentane	3.313	2.741	2.352	2.240	3.213	2.841	2.207
3M-pentane	2.617	2.015	1.556	1.558	2.442	2.267	1.659
2,2-DM-butane	2.413	2.852	0.228	1.408	2.618	6.877	9.375
2,3-DM-butane	0.934	0.871	0.868	0.770	0.965	0.780	0.678
2M-hexane	1.608	1.401	1.242	1.172	1.615	1.429	1.141
3M-hexane	1.767	1.612	1.544	1.394	1.823	1.523	1.265
2,2-DM-pentane	0.350	0.215	0.089	0.128	0.297	0.322	0.194
2,3-DM-pentane	1.324	1.213	1.209	1.061	1.360	1.080	0.912
2,4-DM-pentane	0.861	0.726	0.649	0.577	0.843	0.753	0.589
3,3-DM-pentane	0.240	0.168	0.099	0.115	0.217	0.220	0.145
2,2,3-TM-butane	0.069	0.051	0.035	0.037	0.063	0.062	0.043
2M-heptane	0.596	0.614	0.703	0.587	0.647	0.469	0.457
3M-heptane	0.700	0.722	0.824	0.689	0.759	0.554	0.541
4M-heptane	0.295	0.304	0.345	0.290	0.318	0.236	0.230
2,2-DM-hexane	0.043	0.044	0.050	0.042	0.046	0.034	0.033
2,4-DM-hexane	0.545	0.458	0.519	0.438	0.477	0.352	0.343
2,5-DM-hexane	0.606	0.451	0.518	0.432	0.474	0.343	0.334
3,3-DM-hexane	0.047	0.051	0.058	0.048	0.052	0.037	0.037
2,4-DM-heptane	0.658	0.670	0.733	0.611	0.707	0.496	0.479
3,5-DM-heptane	0.197	0.203	0.233	0.193	0.214	0.156	0.153
2,3-DM-heptane	0.101	0.104	0.119	0.099	0.111	0.080	0.077
3M-octane	0.448	0.460	0.527	0.439	0.484	0.354	0.344
4M-octane	0.168	0.172	0.197	0.164	0.181	0.133	0.129
2,2,4-TM-pentane	6.368	3.947	4.483	3.762	4.168	3.070	2.976
2,3,3-TM-pentane	1.637	1.646	1.876	1.569	1.729	1.265	1.234
2,3,4-TM-pentane	1.518	1.486	1.694	1.418	1.561	1.141	1.112
2,2,5-TM-hexane	0.190	0.196	0.224	0.187	0.207	0.151	0.147
2,3,5-TM-hexane	0.116	0.120	0.137	0.114	0.126	0.092	0.090
Cyclopentane	6.226	6.824	0.762	3.501	6.393	16.146	21.927
M-Cyclopentane	2.269	1.675	1.128	1.211	2.091	2.040	1.407
E-Cyclopentane	0.117	0.121	0.138	0.115	0.127	0.099	0.097
t-1,2-DM-Cyclopentane	0.171	0.165	0.170	0.149	0.180	0.143	0.126

Table A-1. Compositions of CRC-666 fuels (Continued)

CRC 666 Fuel =>	B0	B4	B5	B6	H1	H2	H3
Component	**Wt %**	**Wt %**	**Wt %**	**Wt %**	**Wt %**	**Wt %**	**Wt %**
c-1,3-DM-Cyclopentane	0.732	0.720	0.764	0.660	0.778	0.603	0.548
Cyclohexane	0.653	0.583	0.554	0.506	0.654	0.550	0.452
M-Cyclohexane	0.360	0.379	0.465	0.397	0.391	0.308	0.299
E-Cyclohexane	0.000	0.000	0.000	0.000	0.000	0.000	0.000
c-1,2-DM-Cyclohexane	0.029	0.030	0.034	0.029	0.031	0.023	0.023
c-1,3-DM-Cyclohexane	0.046	0.048	0.055	0.047	0.050	0.036	0.035
t-1,3-DM-Ccyclohexane	0.337	0.341	0.392	0.327	0.360	0.240	0.280
Propene	0.000	0.000	0.000	0.000	0.000	0.000	0.000
1-butene	0.013	0.016	0.017	0.015	0.016	0.000	0.012
c-2-Butene	0.060	0.071	0.077	0.064	0.073	0.052	0.054
t-2-Butene	0.078	0.093	0.100	0.084	0.095	0.067	0.070
2M-propene	0.008	0.010	0.010	0.009	0.009	0.007	0.007
1-pentene	0.092	0.100	0.134	0.000	0.104	0.075	0.075
1-hexene	0.031	0.033	0.044	0.031	0.034	0.027	0.025
2M-2-butene	0.504	0.545	0.605	0.510	0.568	0.413	0.410
Cyclopentadiene	2.808	2.930	3.300	2.743	3.088	2.270	2.203
Benzene	0.383	0.401	0.451	0.382	0.420	0.308	0.300
Toluene	5.489	5.677	6.455	5.402	5.970	4.363	4.253
E-Benzene	0.993	1.023	1.171	0.975	1.079	0.787	0.764
o-Xylene	1.312	1.351	1.546	1.287	1.423	1.039	1.009
m&p-Xylene	3.726	3.839	4.398	3.658	4.048	2.949	2.866
1M-3E-benzene	1.443	1.480	1.701	1.411	1.562	1.140	1.103
1M-4E-benzene	0.465	0.476	0.545	0.455	0.502	0.369	0.357
1,2,3-TM-benzene	0.484	0.466	0.537	0.452	0.502	0.378	0.358
1,2,4-TM-Benzene	1.670	1.696	1.951	1.622	1.796	1.316	1.269
1,3,5-TM-Benzene	0.491	0.503	0.579	0.480	0.532	0.388	0.375
i-Butylbenzene	0.229	0.195	0.225	0.193	0.216	0.170	0.156
s-Butylbenzene	0.044	0.044	0.051	0.042	0.047	0.035	0.033
1,2,3,4-Tetramethylbenzene	0.931	0.563	0.568	0.612	0.712	0.643	0.539
1,2,3,5-Tetramethylbenzene	2.373	1.369	1.610	1.549	1.786	1.670	1.367
1,2,4,5-Tetramethylbenzene	1.701	1.031	1.212	1.157	1.330	1.233	1.015
n-Propylbenzene	0.374	0.384	0.441	0.366	0.405	0.296	0.287
1,3-DE-Benzene	0.172	0.144	0.167	0.145	0.162	0.128	0.117
1M-3-n-Propylbenzene	0.531	0.426	0.496	0.432	0.486	0.392	0.353
1M-4-n-Propylbenzene	0.402	0.292	0.340	0.306	0.345	0.292	0.255
1,2-DE-Benzene	0.912	0.702	0.815	0.718	0.808	0.661	0.591
1M-2-n-Propylbenzene	0.271	0.180	0.210	0.189	0.214	0.182	0.158
1,4-DM-2-E-Benzene	0.775	0.499	0.587	0.536	0.615	0.535	0.454
1,3-DM-4-E-Benzene	0.770	0.504	0.586	0.547	0.622	0.558	0.474
1,2-DM-4-E-Benzene	1.696	1.051	1.229	1.155	1.323	1.197	1.002
1,3-DM-2-E-Benzene	13.396	7.136	8.474	7.852	8.960	7.920	6.765
Ethanol	0.000	11.001	16.891	22.616	0.000	0.000	0.000

Table A-3. Compositions of CRC-638 fuels

CRC 638 Fuel =>	Base	E4	E5	E6	H1	H2	H3
Component	**Wt %**	**Wt %**	**Wt %**	**Wt %**	**Wt %**	**Wt %**	**Wt %**
Propane	0.022	0.018	0.017	0.016	0.022	0.022	0.024
Butane	2.582	1.977	1.999	1.915	2.281	1.998	1.759
Pentane	0.589	0.792	0.590	0.598	0.515	0.483	0.424
Hexane	0.646	0.558	0.550	0.535	1.356	2.561	4.105
Heptane	0.493	0.417	0.404	0.395	0.638	0.926	1.417
Octane	0.239	0.202	0.195	0.193	0.212	0.195	0.171
Nonane	0.093	0.081	0.079	0.077	0.083	0.079	0.070
Decane	0.167	0.102	0.101	0.097	0.149	0.148	0.135
2M-Propane	0.303	0.227	0.231	0.231	0.911	1.239	1.675
2M-Butane	9.912	8.116	7.415	6.886	13.062	11.754	10.628
2,2-DM-propane	0.029	0.026	0.023	0.020	0.037	0.033	0.030
2M-pentane	1.168	1.013	0.974	0.925	1.101	1.091	1.094
3M-pentane	0.789	0.679	0.657	0.627	0.863	1.048	1.295
2,2-DM-butane	0.133	0.113	0.113	0.109	0.119	0.107	0.094
2,3-DM-butane	0.951	0.880	0.783	0.669	0.854	0.773	0.684
2M-hexane	0.588	0.499	0.490	0.489	0.789	1.186	1.728
3M-hexane	0.744	0.639	0.617	0.594	1.001	1.498	2.188
2,2-DM-pentane	0.071	0.060	0.059	0.057	0.066	0.065	0.085
2,3-DM-pentane	1.093	1.057	0.944	0.844	1.098	1.207	1.374
2,4-DM-pentane	0.717	0.623	0.590	0.469	0.645	0.551	0.565
3,3-DM-pentane	0.072	0.061	0.059	0.057	0.090	0.127	0.184
2,2,3-TM-butane	0.055	0.052	0.046	0.039	0.050	0.047	0.047
2M-heptane	0.304	0.263	0.249	0.246	0.271	0.247	0.223
3M-heptane	0.328	0.277	0.267	0.264	0.291	0.266	0.238
4M-heptane	0.179	0.158	0.147	0.145	0.159	0.146	0.131
2,2-DM-hexane	0.029	0.024	0.023	0.023	0.027	0.026	0.029
2,4-DM-hexane	0.795	0.785	0.711	0.630	0.715	0.654	0.586
2,5-DM-hexane	1.029	1.025	0.913	0.795	0.911	0.826	0.729
3,3-DM-hexane	0.026	0.023	0.022	0.022	0.025	0.025	0.027
2,4-DM-heptane	0.722	0.683	0.605	0.581	0.640	0.585	0.521
3,5-DM-heptane	0.116	0.102	0.095	0.097	0.103	0.095	0.085
2,3-DM-heptane	0.061	0.058	0.054	0.057	0.058	0.054	0.047
3M-octane	0.215	0.187	0.176	0.177	0.191	0.176	0.156
4M-octane	0.065	0.059	0.057	0.057	0.058	0.053	0.051
2,2,4-TM-pentane	12.807	12.666	12.229	10.592	11.301	10.288	9.133
2,3,3-TM-pentane	2.810	2.755	2.406	2.293	2.492	2.266	2.004
2,3,4-TM-pentane	2.697	2.654	2.345	2.161	2.393	2.176	1.924
2,2,5-TM-hexane	0.726	0.699	0.594	0.599	0.644	0.588	0.521
2,3,5-TM-hexane	0.654	0.778	0.609	0.961	0.664	0.544	0.485
Cyclopentane	0.084	0.075	0.061	0.074	0.076	0.069	0.061
M-Cyclopentane	0.294	0.253	0.248	0.239	0.414	0.633	0.917
E-Cyclopentane	0.039	0.036	0.035	0.030	0.045	0.059	0.087
t-1,2-DM-Cyclopentane	0.046	0.045	0.045	0.037	0.078	0.126	0.194

Table A-4. Compositions of CRC-638 fuels (Continued)

CRC 638 Fuel =>	Base	E4	E5	E6	H1	H2	H3
Component	**Wt %**	**Wt %**	**Wt %**	**Wt %**	**Wt %**	**Wt %**	**Wt %**
c-1,3-DM-Cyclopentane	0.438	0.374	0.349	0.345	0.493	0.597	0.766
Cyclohexane	0.061	0.058	0.061	0.060	0.071	0.092	0.217
M-Cyclohexane	0.162	0.140	0.138	0.131	0.195	0.265	0.407
E-Cyclohexane	0.014	0.020	0.013	0.012	0.013	0.012	0.011
c-1,2-DM-Cyclohexane	0.017	0.014	0.013	0.013	0.015	0.013	0.012
c-1,3-DM-Cyclohexane	0.023	0.020	0.019	0.019	0.020	0.018	0.017
t-1,3-DM-Ccyclohexane	0.291	0.263	0.243	0.258	0.274	0.238	0.213
Propene	0.015	0.008	0.009	0.010	0.012	0.010	0.009
1-butene	0.032	0.023	0.024	0.024	0.027	0.024	0.021
c-2-Butene	0.092	0.072	0.072	0.070	0.082	0.071	0.062
t-2-Butene	0.086	0.066	0.067	0.065	0.075	0.066	0.057
2M-propene	0.029	0.022	0.023	0.022	0.026	0.022	0.020
1-pentene	0.087	0.072	0.072	0.068	0.078	0.070	0.060
1-hexene	0.030	1.649	2.796	0.025	0.027	0.025	0.021
2M-2-butene	4.385	7.685	4.833	4.058	3.905	7.354	6.312
Cyclopentadiene	0.043	0.078	0.033	0.067	0.038	0.075	0.029
Benzene	0.994	0.838	0.812	0.791	0.886	0.798	0.697
Toluene	7.547	8.180	7.844	7.737	6.692	6.091	5.377
E-Benzene	0.750	0.477	0.462	0.459	0.665	0.613	0.545
o-Xylene	1.416	1.058	1.027	1.024	1.305	1.255	1.174
m&p-Xylene	3.410	2.303	2.234	2.223	3.072	2.883	2.620
1M-3E-benzene	6.971	7.276	7.051	7.048	7.482	8.097	8.608
1M-4E-benzene	1.945	2.026	1.977	1.974	2.046	2.199	2.268
1,2,3-TM-benzene	1.400	1.515	1.490	1.439	1.451	1.553	1.620
1,2,4-TM-Benzene	7.657	7.997	7.780	7.759	8.045	8.714	9.202
1,3,5-TM-Benzene	2.136	2.223	2.161	2.159	2.244	2.428	2.566
i-Butylbenzene	0.154	0.165	0.158	0.167	0.157	0.167	0.173
s-Butylbenzene	0.134	0.148	0.145	0.139	0.143	0.155	0.165
1,2,3,4-Tetramethylbenzene	0.699	0.775	0.781	0.747	0.648	0.659	0.645
1,2,3,5-Tetramethylbenzene	1.081	1.205	1.241	1.265	0.955	0.900	0.807
1,2,4,5-Tetramethylbenzene	0.776	0.859	0.885	0.910	0.687	0.655	0.589
n-Propylbenzene	1.452	1.511	1.466	1.465	1.525	1.645	1.736
1,3-DE-Benzene	0.327	0.377	0.378	0.358	0.324	0.336	0.338
1M-3-n-Propylbenzene	0.839	0.946	0.948	0.958	0.810	0.824	0.810
1M-4-n-Propylbenzene	0.670	0.754	0.765	0.753	0.635	0.638	0.616
1,2-DE-Benzene	1.268	1.104	1.389	1.397	1.223	1.207	1.223
1M-2-n-Propylbenzene	0.310	0.350	0.355	0.357	0.289	0.286	0.272
1,4-DM-2-E-Benzene	0.644	0.676	0.690	0.731	0.589	0.576	0.537
1,3-DM-4-E-Benzene	0.586	0.620	0.631	0.679	0.532	0.518	0.479
1,2-DM-4-E-Benzene	1.095	1.100	1.203	1.260	0.988	0.811	0.672
1,3-DM-2-E-Benzene	4.452	0.000	2.440	5.246	3.758	0.000	0.102
Ethanol	0.000	3.156	6.095	9.786	0.000	0.000	0.000

Appendix B

Description of Computer Program (CRCdriveability) for Predicting Fuel Vaporization in a Cold Combustion System using the Thermodynamic Model

The computer program (CRCdriveability) consists of several components and execution steps as shown in schematic diagram Figure B-1. Screen shots of program windows are shown in Figures B-2 and B-3. All the steps involved in using the program (also shown in Figures B-1, B-2, and B-3) are described below.

Step 1. When the program is started by clicking on **CRCdriveability.exe** file, the main program window with menu options opens as shown in Figure B-2. Note that the program shows a copyright message and asks the user to select a name for the output data file before opening the main program window.

Step 2. When the menu option **Cold Start Estimation** is selected, the program opens a MS File Explorer window as shown in Figure B-2 for selecting test fuel composition data file. When a fuel composition data file is selected, the program opens the file and reads all component names and concentrations (Wt%). The program compares fuel components with the database to make sure all the components are valid. If there are any invalid components, it displays a message and ignores the invalid components by normalizing the other component concentrations to 100%.

Step 3. The program provides the option to splash blend the selected fuel with ethanol. This option was used for preparing CRC fuels B1, B2, B3, E1, E2, and E3 as mentioned in Appendix A.

Step 4. The program opens an oxygenate blending dialog box as shown in Figure B-2. Note that the program provides the option to blend with various oxygenates; however, only ethanol was used for this project. After entering the ethanol concentration (vol %), the program computes the DVPE of the blend.

Step 5. The program opens the final dialog box (Figure B-2) for estimating fuel vaporization and various other properties. The user selects temperature and fuel injection amount (cc per liter of air) and clicks on **Compute the Following.** The program performs all of the calculations and displays the results in the dialog box. The program also saves all the results including fuel and vapor compositions in an output.dat file as shown in Figure B-3.

Step 5 can be repeated by changing the input temperature and fuel injection amount, so that the results can be used for plotting the fuel vaporization as a function of temperature. Figure B-4 shows an example of a predicted fuel vaporization plot for the same fuel (CRC-666 fuel B0+10%ethanol) used in all the illustrations in this Appendix. Similar plots were prepared for various other CRC-666 and CRC-638 fuels to study the mechanism of ethanol effects on cold-start and warm-up driveability. Note that fuel vaporizations were not predicted above about 70% fuel vaporized because there was no need for it in this study. Also, the estimation of fuel vaporization >70% requires accurate measurement of heavy component concentrations. The compositions of heavy fuel components were only approximate due to the large number of unknown heavy components and known heavy components with unavailable data as explained in Appendix A.

Figure B-1. Flow Chart of Computer Program CRCdriveability

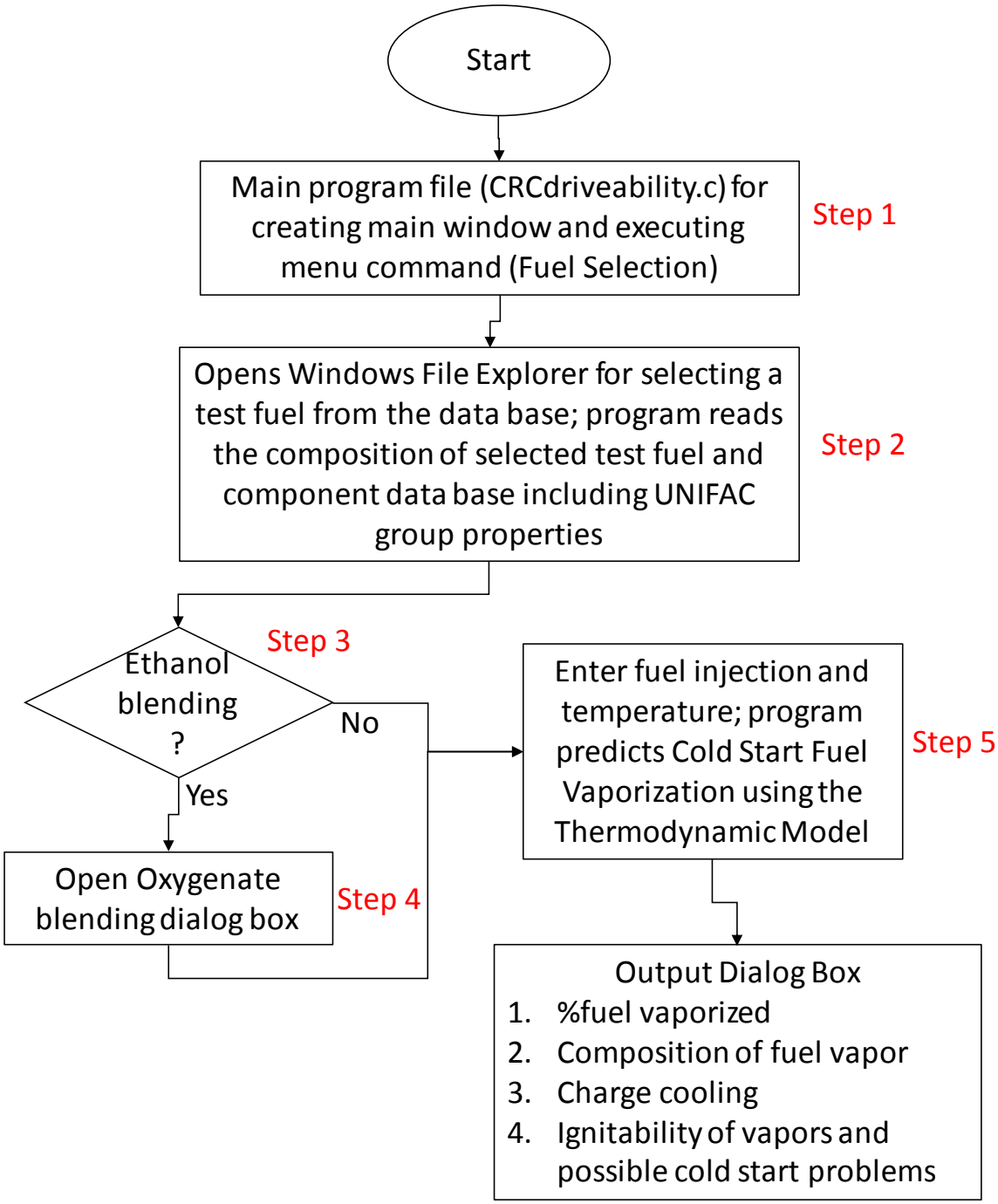

Figure B-2. Screen Shots of Computer Program (CRCdriveability) Steps 1-5

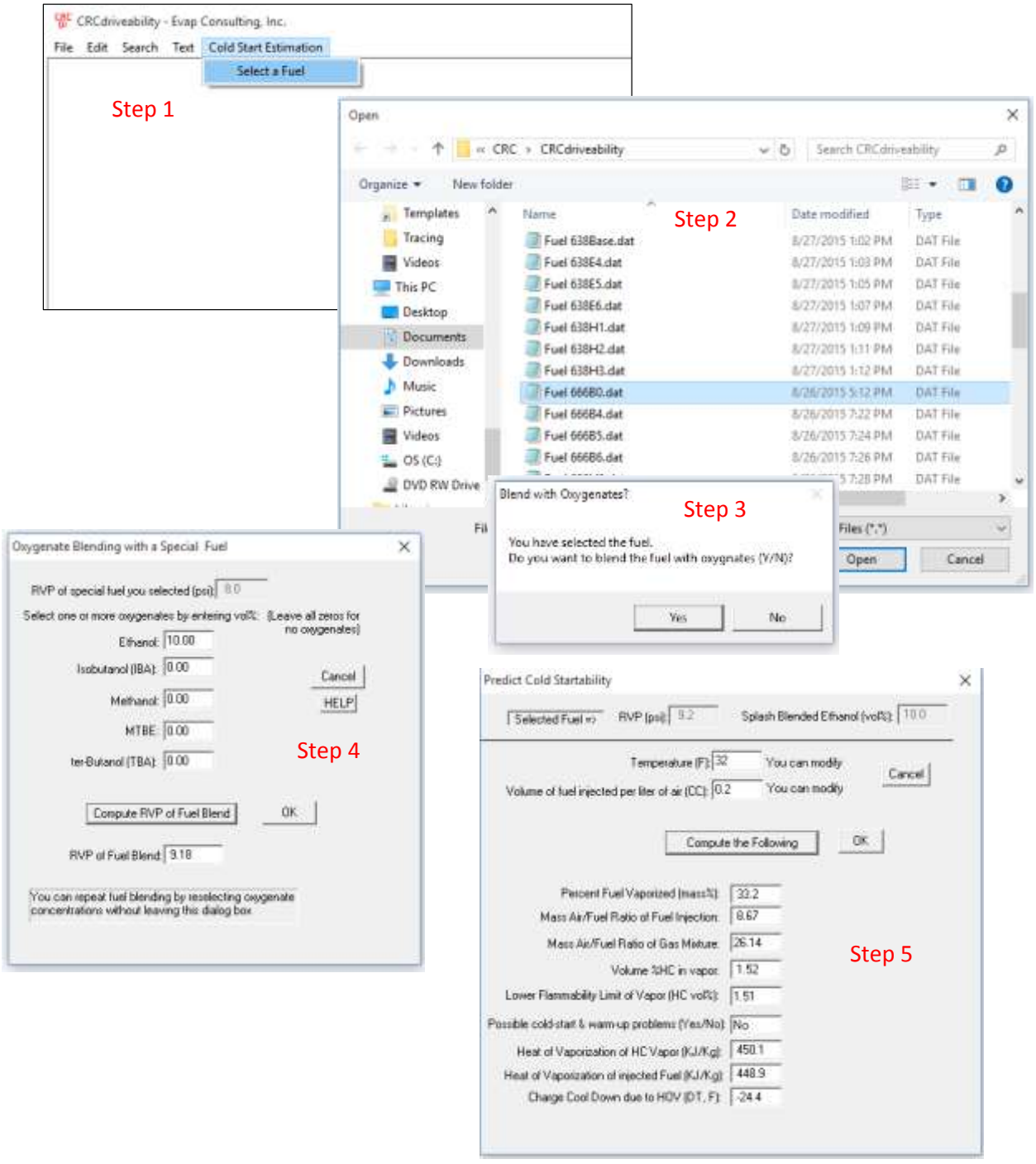

Figure B-3. Screen Shot of output.dat file

```
Fuel RVP =     9.18 psi
Amount of fuel injection per liter of air (cc) =   0.200
Initial Temperature of fuel and air (F) =    32.0
********** Vapor/Liquid Equilibrium Calculations **********
Component                      Mass Percent in Fuel  Mass Percent in Un-vaporized Fuel  Mass Percent in vpr
_____                          ____________________  ___________________________________  ___________________
Propane                                       0.002                                0.00                 0.01
2M-Propane                                    2.039                                0.00                 6.15
2M-Propene                                    0.007                                0.00                 0.02
1-Butene                                      0.012                                0.00                 0.04
Butane                                        0.658                                0.00                 1.98
t-2-Butene                                    0.070                                0.00                 0.21
2,2-DM-Propane                                0.003                                0.00                 0.01
c-2-Butene                                    0.054                                0.00                 0.16
Ethanol                                      10.528                                9.41                12.77
Isobutanol                                    0.002                                0.00                 0.00
2M-Butane                                     3.222                                0.03                 9.64
1-Pentene                                     0.082                                0.00                 0.24
Pentane                                       1.280                                0.06                 3.73
2M-2-Butene                                   0.451                                0.04                 1.27
Cyclopentadiene                               2.512                                0.02                 5.93
2,2-DM-Butane                                 2.159                                0.36                 5.78
Cyclopentane                                  5.570                                1.40                13.97
2,3-DM-Butane                                 0.836                                0.29                 1.94
2M-Pentane                                    2.964                                1.24                 6.44
3M-Pentane                                    2.341                                1.14                 4.76
1-Hexene                                      0.028                                0.02                 0.05
Hexane                                        3.695                                2.38                 6.34
2,2-DM-Pentane                                0.313                                0.26                 0.42
M-Cyclopentane                                2.030                                1.47                 3.15
2,4-DM-Pentane                                0.770                                0.68                 0.96
2,2,3-TM-Butane                               0.062                                0.05                 0.08
Benzene                                       0.343                                0.34                 0.34
3,3-DM-Pentane                                0.215                                0.20                 0.24
Cyclohexane                                   0.584                                0.54                 0.67
3,3-DM-Pentane                                0.215                                0.20                 0.24
Cyclohexane                                   0.584                                0.54                 0.67
2M-Hexane                                     1.439                                1.56                 1.20
2,3-DM-Pentane                                1.185                                1.25                 1.05
3M-Hexane                                     1.581                                1.76                 1.23
c-1,3-DM-Cyclopentane                         0.655                                0.71                 0.55
t-1,2-DM-Cyclopentane                         0.153                                0.17                 0.12
2,2,4-TM-Pentane                              5.697                                6.65                 3.78
Heptane                                       0.944                                1.15                 0.53
M-Cyclohexane                                 0.322                                0.39                 0.19
2,2-DM-Hexane                                 0.038                                0.05                 0.02
2,5-DM-Hexane                                 0.542                                0.71                 0.20
E-Cyclopentane                                0.105                                0.12                 0.07
2,4-DM-Hexane                                 0.488                                0.64                 0.18
3,3-DM-Hexane                                 0.042                                0.06                 0.02
2,3,4-TM-Pentane                              1.358                                1.78                 0.58
2,3,3-TM-Pentane                              1.465                                1.95                 0.40
Toluene                                       4.911                                6.61                 1.48
2M-Heptane                                    0.533                                0.74                 0.12
4M-Heptane                                    0.264                                0.36                 0.06
3M-Heptane                                    0.626                                0.87                 0.14
c-1,3-DM-Cyclohexane                          0.041                                0.06                 0.01
2,2,5-TM-Hexane                               0.170                                0.24                 0.03
Octane                                        0.393                                0.56                 0.05
t-1,3-DM-Ccyclohexane                         0.302                                0.42                 0.06
2,3,5-TM-Hexane                               0.104                                0.15                 0.01
2,4-DM-Heptane                                0.589                                0.85                 0.05
c-1,2-DM-Cyclohexane                          0.026                                0.04                 0.00
3,5-DM-Heptane                                0.176                                0.26                 0.01
E-Benzene                                     0.888                                1.29                 0.07
2,3-DM-Heptane                                0.090                                0.13                 0.01
m&p-Xylene                                    3.334                                4.87                 0.24
4M-Octane                                     0.150                                0.22                 0.01
3M-Octane                                     0.401                                0.59                 0.02
o-Xylene                                      1.174                                1.73                 0.06
Nonane                                        0.167                                0.25                 0.01
n-Propylbenzene                               0.335                                0.50                 0.01
1M-3E-Benzene                                 1.291                                1.92                 0.02
1M-4E-Benzene                                 0.416                                0.62                 0.01
1,3,5-TM-Benzene                              0.439                                0.65                 0.01
1,2,4-TM-Benzene                              1.494                                2.23                 0.01
Decane                                        0.752                                1.12                 0.01
1-Butylbenzene                                0.205                                0.31                 0.00
s-Butylbenzene                                0.039                                0.06                 0.00
1,2,3-TM-Benzene                              0.433                                0.65                 0.00
1,3-DE-Benzene                                0.154                                0.23                 0.00
1M-3-n-Propylbenzene                          0.475                                0.71                 0.00
1M-4-n-Propylbenzene                          0.360                                0.54                 0.00
1,2-DE-Benzene                                0.816                                1.22                 0.00
1M-2-n-Propylbenzene                          0.242                                0.36                 0.00
1,4-DM-2-E-Benzene                            0.693                                1.04                 0.00
1,3-DM-4-E-Benzene                            0.689                                1.03                 0.00
1,2-DM-4-E-Benzene                            1.517                                2.27                 0.00
1,3-DM-2-E-Benzene                           11.985                               17.92                 0.04
1,2,4,5-Tetramethylbenzene                    1.522                                2.28                 0.00
1,2,3,5-Tetramethylbenzene                    2.123                                3.18                 0.00
1,2,3,4-Tetramethylbenzene                    0.833                                1.25                 0.00
Amount of fuel injection per liter of air (cc) =   8.200
Initial Temperature of fuel and air (F)        =    32.0
Percent of injected fuel vaporized   =  33.2
Mass air/fuel ratio of injected fuel =  8.67
Mass air/fuel ratio of fuel vapors   = 26.14
Percent HC in vapors                 =  1.52
Lower Flammability of vapors         =  1.51
Heat of vaporization of liquid fuel(KJ/Kg) =  448.9
Heat of vaporization of vapor fuel(KJ/Kg)  =  450.1
Adiabatic charge cooling (DT, deg F) =  -24.6
```

Figure B-4. An Example of Predicted Fuel Vaporization in Combustion System as a Function of Temperature

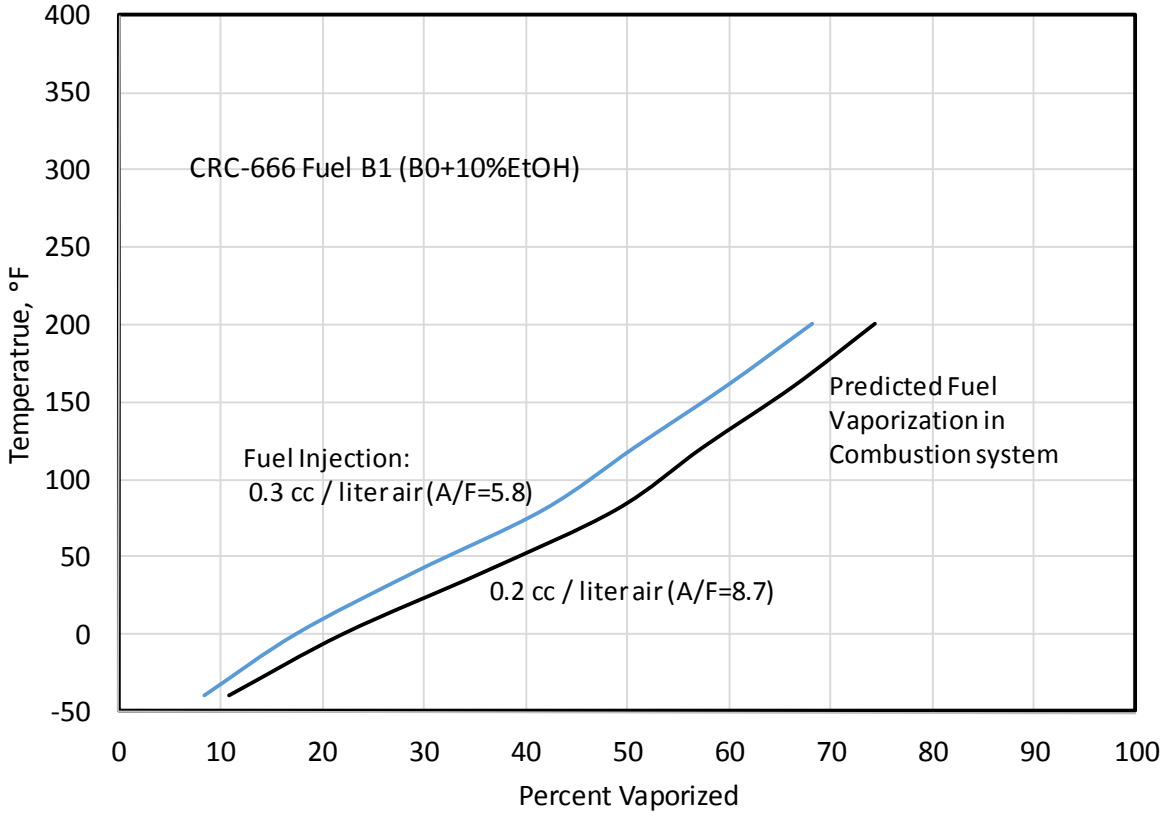

Appendix C
Estimation of Ethanol Blend T50 Depression using Equation:

$$\Delta T50 = \Delta T50_{avg} + \Delta T50_{Deviation} = \Delta T50_{avg} + f(T50_{Blend}, EtOH)$$

As described in the report, a simple correlation equation was developed for estimating ΔT50 involving $\Delta T50_{avg}$ and a correction factor F which is a function of blend T50. Another correlation equation involving both blend T50 and ethanol concentration (EtOH) is developed in this Appendix. API data were analyzed to develop equations for estimating $\Delta T50_{Deviation}$ using the blend T50 and EtOH. For all the blends, $\Delta T50_{Deviation}$ was computed and plotted as a function of blend T50 for each ethanol concentration as shown in Figure C-1. Correlation equations between blend T50 and $\Delta T50_{Deviation}$ and their corresponding correlation coefficients are also shown in the plots in Figure C-1. In all cases, straight trendline was selected purposely so that a single equation for all the blends for estimating $\Delta T50_{Deviation}$ can be developed as illustrated below. The correlation equations in Figure C-1 show that the slope (m) of the trendline increases with ethanol concentration and the intercept (b) of the trendline decreases with ethanol concentration. Therefore, the trendline slopes and intercepts were plotted as a function of ethanol concentration as shown in Figures C-2a and C-2b. A second order polynomial trendline was selected in both the plots as shown in Figure C-2a & C-2b, and summarized below. Note that it was necessary to select zero intercept for the trendline so that ΔT50 becomes negligible when EtOH=0.

$$\Delta T50 = \frac{51}{1+114e^{-0.5\,EtOH}} + m\,(T50) + b \qquad \text{(C-1)}$$

Where slope $m = 0.007*EtOH^2 - 0.0358*EtOH$ and intercept $b = -1.1951*EtOH^2 + 7.1716*EtOH$

Equation (C-1) can be written as:

$$\Delta T50 = \frac{51}{1+114e^{-0.5\,EtOH}} + (0.007*EtOH^2 - 0.0358*EtOH)\,(T50) + (-1.1951*EtOH^2 + 7.1716*EtOH) \qquad \text{(C-2)}$$

Once again, API data were used to determine correlation between measured T50 depression ($\Delta T50_{Measured}$) and T50 depression ($\Delta T50_{Predicted}$) predicted by Equation (C-2). The results are shown in Figure C-3. Poor correlation is mainly due to E10-E20 blends. The trendlines in Figure C-2a and Figure C-2b deviated significantly for E10-E20 blend when the trendlines were forced through the origin.

The CRC-666 driveability data were re-analyzed by re-computing $DI_{\Delta T50}$ using Equation (C-2) for ΔT50 estimation and the results are shown in Figure C-4. Unfortunately, correlation between $DI_{\Delta T50}$ and driveability performance was better (R^2=0.8733 in Figure 12) when $\Delta T50=\Delta T50_{avg}$ was used, compared to the correlation when $\Delta T50_{Deviation}$ is used (R^2=0.791 in Figure C-4). The reason for deterioration in the correlation appears to be that $\Delta T50_{avg}$ is a better estimate of T50 depression for CRC-666 fuels, compared to ΔT50 estimation by applying $\Delta T50_{Deviation}$ which is based on a weak correlation equation.

Figure C-1. ΔT50 Deviations of Various Ethanol Blends as function Blend T50

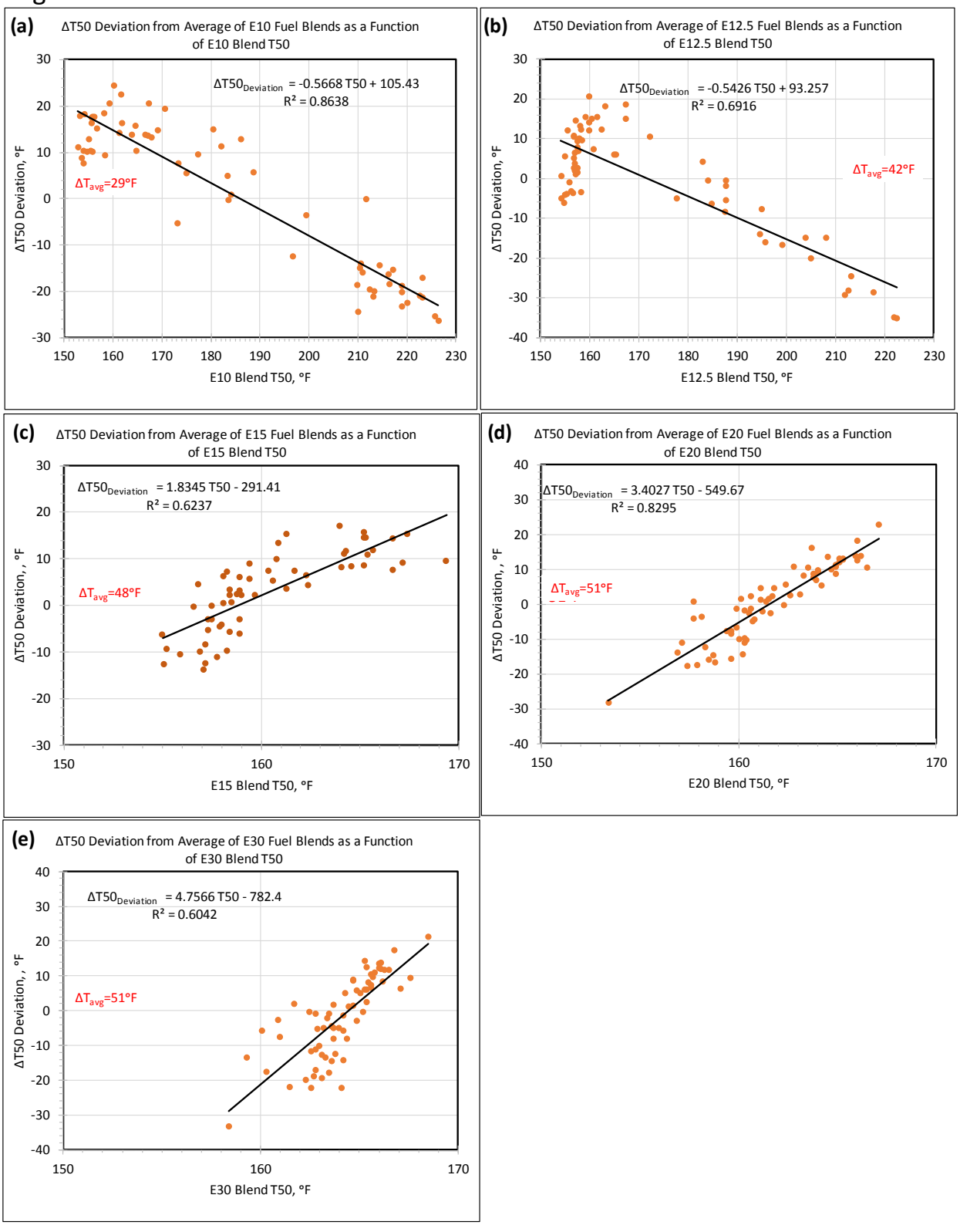

Figure C-2a. Slope of Correlation Equation $\Delta T50_{Deviation} = m(T50)+b$

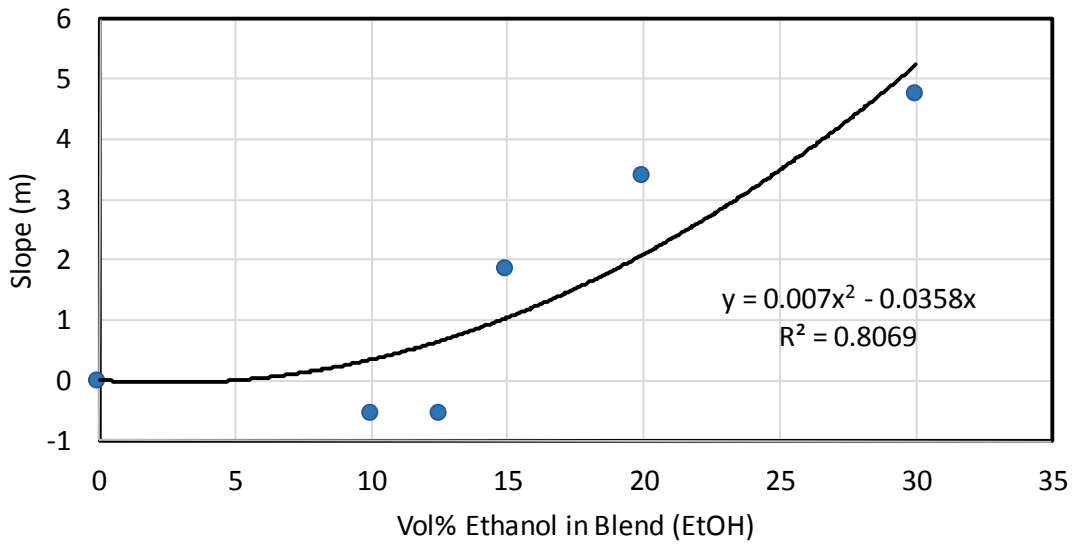

Figure C-2b. Intercept of Correlation Equation $\Delta T50_{Deviation} = m(T50)+b$

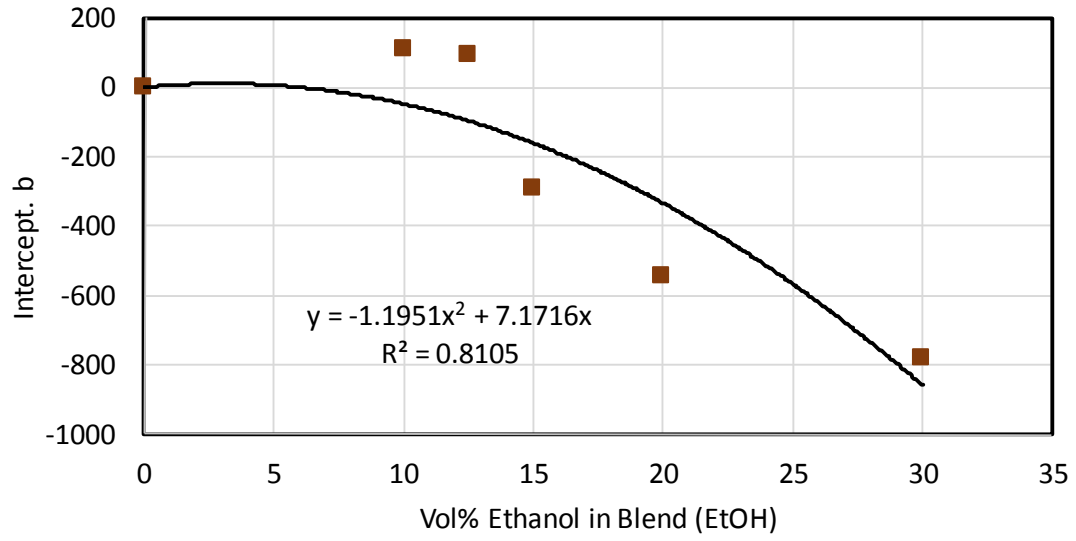

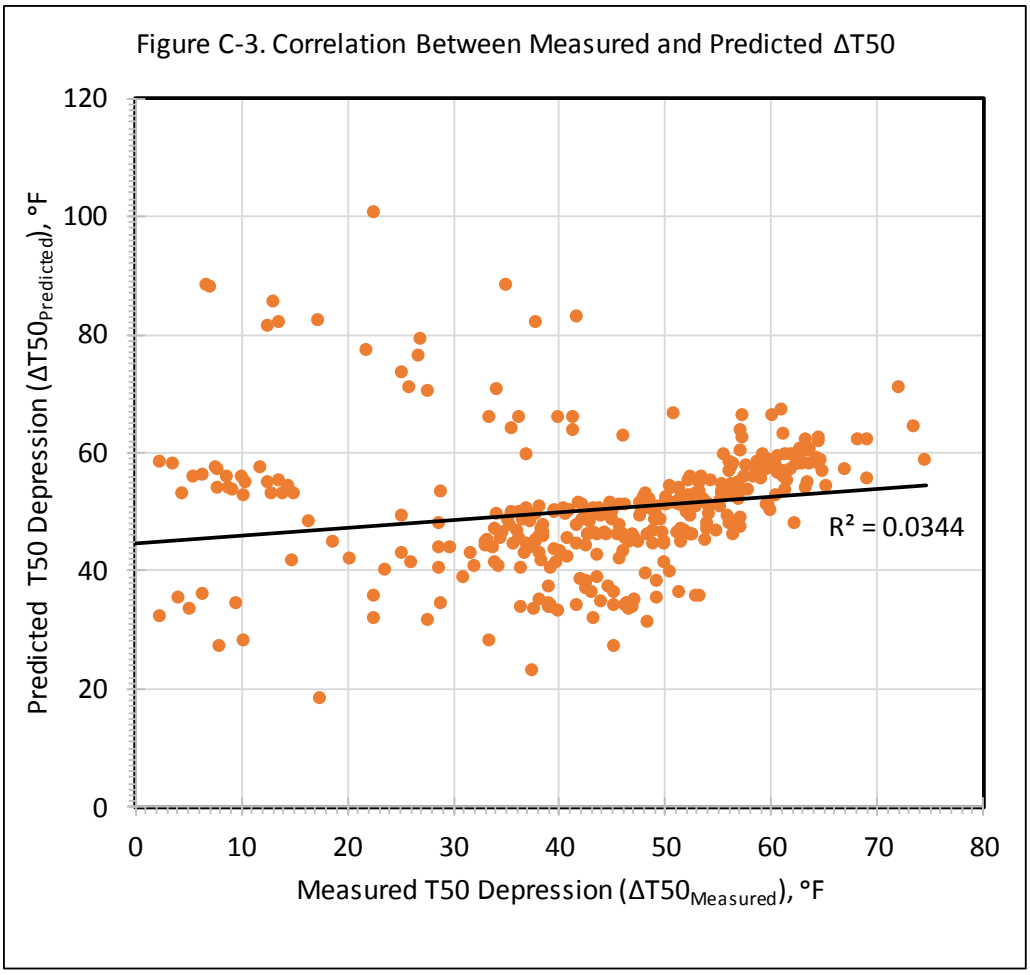
Figure C-3. Correlation Between Measured and Predicted ΔT50
Predicted T50 Depression (ΔT50Predicted), °F
Measured T50 Depression (ΔT50Measured), °F
R² = 0.0344
0
20
40
60
80
100
120
0
10
20
30
40
50
60
70
80

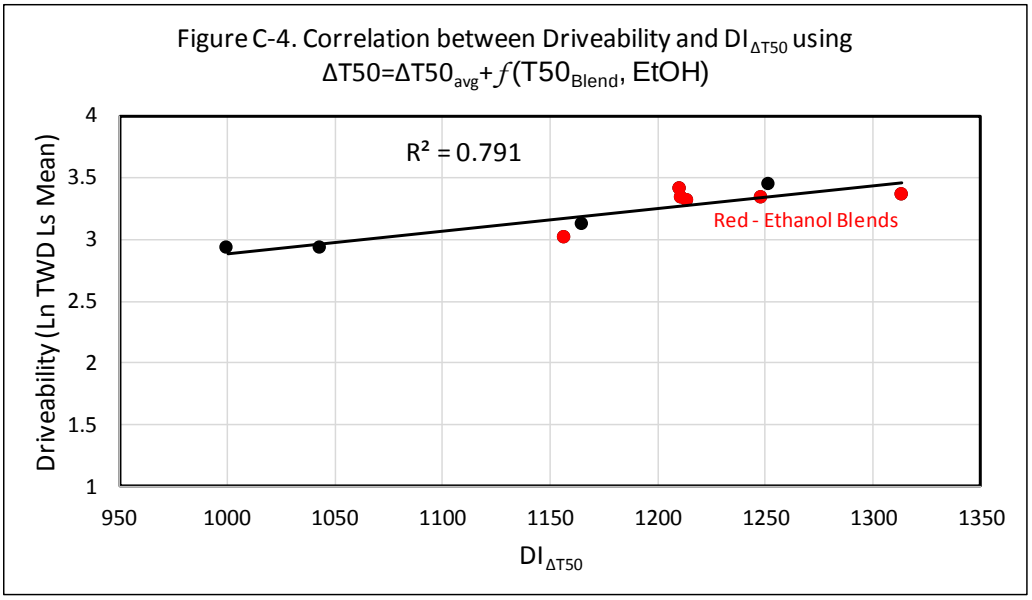
Figure C-4. Correlation between Driveability and DIΔT50 using
ΔT50=ΔT50avg+f(T50Blend, EtOH)
Driveability (Ln TWD Ls Mean)
DIΔT50
R² = 0.791
Red - Ethanol Blends
1
1.5
2
2.5
3
3.5
4
950
1000
1050
1100
1150
1200
1250
1300
1350

Appendix D

Estimation of the BOB DI_{E0} from its Gasoline-ethanol Blend DI_{E0}

Based on the thermodynamic model, a revised driveability index $DI_{\Delta T50}$ was proposed for ethanol blends, which requires the estimation of T50 depression (ΔT50) ($DI_{\Delta T50}$=1.5T50+3T50+T90+3ΔT50). Another option is to use base fuel or DI_{E0} of BOB for estimating of $DI_{\Delta T50}$ ($DI_{\Delta T50}=DI_{E0\_BOB}$). For any given ethanol blend, DI_{E0_BOB} may or may not be available; however, it can be estimated from DI_{E0_Blend} (uncorrected DI of ethanol blend) as described by the following equation.

$$DI_{\Delta T50} = DI_{E0\_BOB} = f(DI_{E0\_Blend,}\ EtOH) \qquad \text{(D-1)}$$

To find correlation equations between DI_{E0_BOB} and DI_{E0_Blend}, DI_{E0_BOB} of all the API base stocks (BOBs) and DI_{E0_Blend} of various ethanol blends were computed and plotted as shown in Figure D-1. The correlation coefficients for each of the blends (shown in Figure D-1) show good correlation ($R^2 \geq 0.85$) between blend DI_{E0_Blend} and $DI_{E0\_BOB,}$ which indicates that $DI_{\Delta T50}$ can be estimated from $DI_{E0\_Blend.}$ However, the problem with this method of $DI_{\Delta T50}$ estimation is that it requires a separate correlation equation for each ethanol concentration. For example, if the ethanol concentration is 17%, none of the correlation equations shown in Figure D-1 can be used for estimating $DI_{\Delta T50}$.

CRC-666 driveability data were re-analyzed by estimating the DI_{E0_BOB} of ethanol containing fuels B1 through B6 using the correlation equation (shown in Figure D-1) and the results as shown in Figure D-2. Note that for hydrocarbon fuels (fuels H1, H2, and H3), DI_{E0_BOB} is nothing but DI_{E0} of the fuel. The correlation between estimated DI_{E0_BOB} and driveability is reasonably good (R^2=0.8233); however, it may not be an attractive method for $DI_{\Delta T50}$ because of the inconvenience of a separate equation for each ethanol concentration.

Figure D-1. Correlation between DI_0 of Ethanol Blends and DI_{0_BOB}

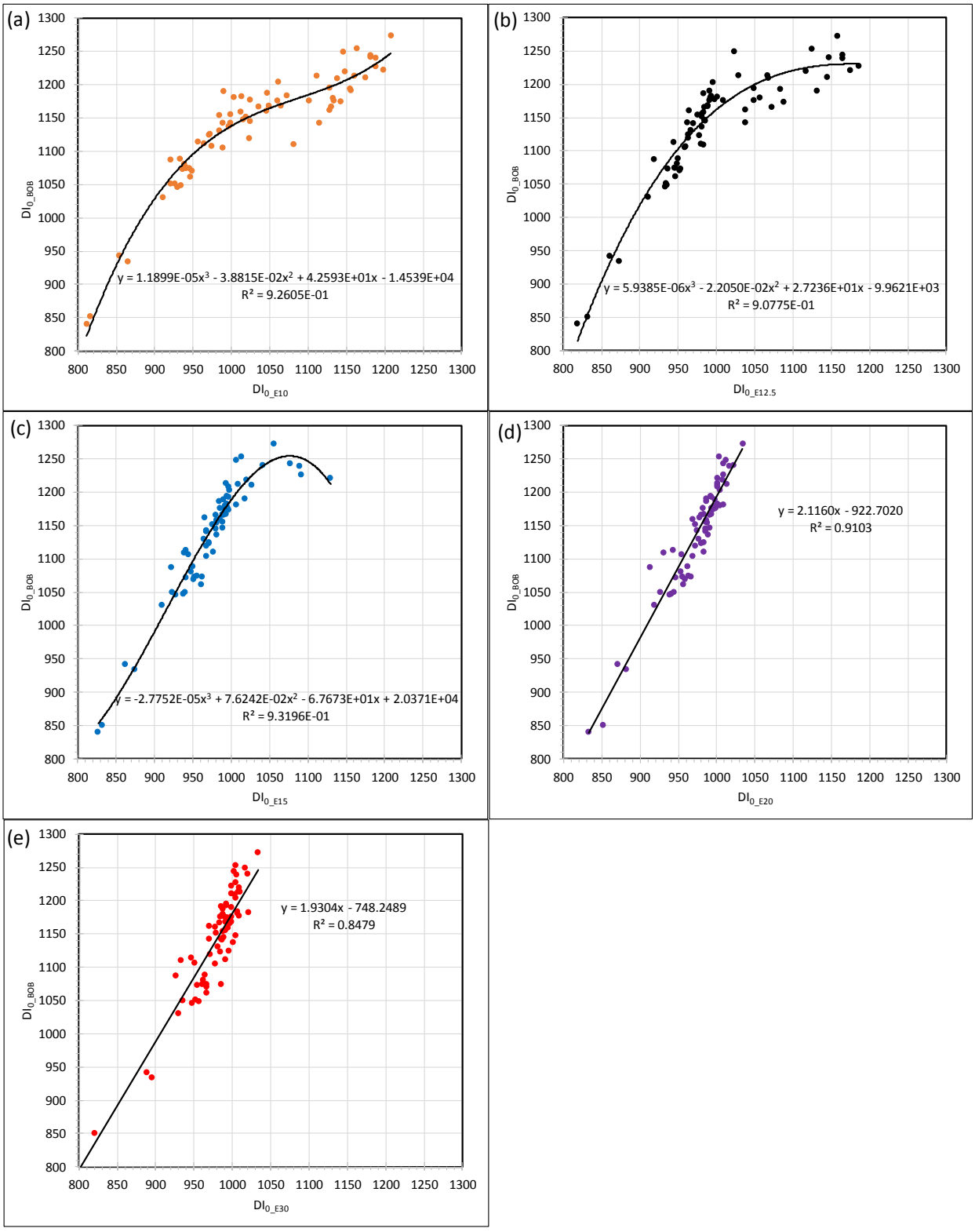

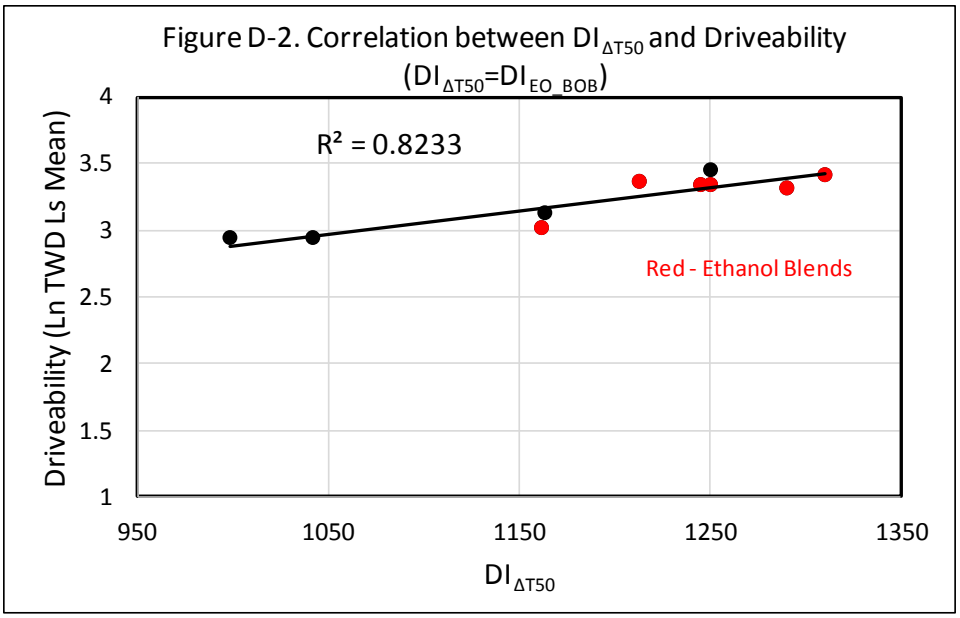
Figure D-2. Correlation between DI ΔT50 and Driveability
(DI ΔT50=DI EO_BOB)
R² = 0.8233
Red - Ethanol Blends
Driveability (Ln TWD Ls Mean)
DI ΔT50
4
3.5
3
2.5
2
1.5
1
950
1050
1150
1250
1350